Received: 25 February 2019 | Revised: 4 June 2019 | Accepted: 6 June 2019

DOI: 10.1002/wcms.1432

ADVANCED REVIEW

WIREs COMPUTATIONAL MOLECULAR SCIENCE WILEY

Quasistructural molecules

Attila G. Császár[1,2] | **Csaba Fábri**[1,2] | **János Sarka**[3]

[1]Laboratory of Molecular Structure and Dynamics, Institute of Chemistry, ELTE Eötvös Loránd University, Budapest, Hungary

[2]MTA-ELTE Complex Chemical Systems Research Group, Budapest, Hungary

[3]Department of Chemistry and Biochemistry, Texas Tech University, Lubbock, Texas, USA

Correspondence
Attila G. Császár, Laboratory of Molecular Structure and Dynamics, Institute of Chemistry, ELTE Eötvös Loránd University, H-1117 Budapest, Pázmány Péter sétány 1/A, Hungary.
Email: csaszarag@caesar.elte.hu

Funding information
NKFIH, Grant/Award Numbers: K119658, PD124699; European Regional Development Fund, Grant/Award Number: VEKOP-2.3.2-16-2017-00014

Abstract

The concept of quasistructural molecules is introduced. For quasistructural molecules (a) the notion of a static equilibrium structure, corresponding to a minimum on the potential energy surface of the molecule, loses its strict meaning, (b) internal nuclear motions (rotations and vibrations) become dominant, resulting in an effective molecular structure often even qualitatively different from the equilibrium one, (c) separation of the internal nuclear motions breaks down, rotational and vibrational degrees of freedom cannot be separated from each other when interpreting even the lowest rovibrational eigenstates of the molecule, often resulting in effective rotational constants drastically different from the equilibrium ones even for the ground vibrational eigenstate, (d) classification of the rovibrational states requires the use of permutation-inversion symmetry and molecular-symmetry groups, and (e) some of the rovibrational eigenenergies assigned to a vibrational parent state exhibit unconventional (in the most striking cases "negative") rotational contributions. Molecules showing quasistructural behavior include neutral species, such as dimethyl acetylene, charged species, such as H_5^+ and CH_5^+, van der Waals complexes, such as $CH_4{\cdot}H_2O$, and molecular complexes held together by halogen bonds, like $CF_3Cl{\cdot}CH_3F$.

This article is categorized under:

Structure and Mechanism > Molecular Structures

Theoretical and Physical Chemistry > Spectroscopy

Software > Quantum Chemistry

KEYWORDS

nuclear motion computation, quasistructural molecules, molecular-symmetry groups, quantum dynamics, internal motions

1 | OF MOLECULES AND STRUCTURES

"Molecule" and "structure" are two fundamental concepts helping the description of the quantum world surrounding us. Nevertheless, when attempting to provide a strict definition of these two terms one runs into considerable difficulties. A substantial part of the difficulties arises from the fact that neither of these classical concepts (especially not that of "molecular structure") are particularly well defined within quantum mechanics.[1–9]

Löwdin[10] provided the following definition of a "molecule": "A system of electrons and atomic nuclei is said to form a molecule if the Coulombic Hamiltonian—with the center of mass motion removed—has a discrete ground state energy, E_0." This is a fine definition and one can greatly elaborate on this, as was done first by Löwdin[10] and later by Sutcliffe.[11] Löwdin himself[10] added: "We have further observed that almost all atomic and molecular applications are based on the *conjecture* that, if one can find an expectation value of the Hamiltonian … which is lower than the lowest energy of all separated clusters, the ground state is a bound state associated with a discrete eigenvalue E_0."

There are, of course, other available definitions for "molecule." Upon first reading, the Gold Book[12] of the International Union of Pure and Applied Chemistry (IUPAC) provides a seemingly similar definition: "a molecule is an electronically neutral entity consisting of more than one atom … and it must correspond to a depression on the potential energy surface (PES) that is deep enough to confine at least one vibrational state." This definition, while indeed similar to the one offered by Löwdin,[10] appears to be less satisfactory. First, it refers to the charge of the molecular system which could (and perhaps should) be left out of the definition. Second, it uses the concept of a PES, in other words a clamped-nuclei electronic potential,[8] for the definition of a molecule, whereas molecules do exist outside of the realm of PESs, as PESs arise only within the adiabatic separation of nuclear and electronic degrees of freedom (dof). In fact, for nonrelativistic three-particle Coulombic quantum systems the emergence of the notion of a molecule was shown "to result from the inherent nature of the physical theory."[9] Third, the Coulombic interaction, upon which the usual (nonrelativistic) Hamiltonians of chemistry are based, is left out of the definition. Fourth, Löwdin deliberately leaves out internal nuclear motions from the definition, while IUPAC singles out vibrations, only one form of the nuclear motions of a molecular system. It is left to the experts of IUPAC to redefine what a "molecule" is. Here we only note that the earlier definition of Löwdin[10] appears to capture better our present-day understanding of a "molecule."

Next, let us consider the definition of "structure." For most chemists, structure basically means equilibrium structure,[13] r_e, defined within the adiabatic (much more often the venerable Born–Oppenheimer (BO)[1,2,14]) separation of the nuclear and electronic dofs: they correspond to minima ("depressions") on the PES of the molecule.[15,16] This is a very clear and a seemingly unambiguous, in fact "classical-like"[17] definition and it is independent, in its simplest form, from actual measurements. While this definition has a number of advantages,[13] there is a problem with identifying the structure of a molecule with its static equilibrium structure: this choice introduces no dynamical (rotational–vibrational) information into the definition. This is fine for the great majority of molecules chemists must deal with but becomes an issue when complications introduced by nuclear motions (note also the case of systems distorted by the Jahn–Teller (JT) effect,[18–21] that is, the case when one needs to move beyond the adiabatic separation of electronic and nuclear motions for certain high(er)-symmetry open-shell systems) become overwhelmingly important, as it happens for certain molecular systems. In fact, these exceptional closed-shell molecular systems form the topic of this review. It must be added that there are many structures other than the "equilibrium" one defined in the literature.[6,13] The large number of temperature-dependent, rovibrationally averaged structures (position (r_z, $r_{\alpha,T}$) and distance (angle) averages ($r_{g,T}$, $r_{a,T}$), as well as mass-dependent (r_m) and empirical (r_0, r_s) ones),[6,13,22–24] though they correspond much more closely to what one might call "measured" structures, are not considered in this review, as they are also based on the BO approximation when computed and thus they do not enhance the present discussion.

An alternative concept and definition of "structure" is offered by quantum statistical mechanics via its time-dependent many-body density matrix involving all the nuclei and the electrons of the system.[25,26] Taking the trace of the density matrix over all electrons at a certain time and a suitable time averaging helps one to arrive at experimentally accessible "structures" through this advanced formalism. This approach does not rely on the concept of equilibrium structures of molecules, which is one of its considerable advantages. However, it does not yield information about high-resolution spectra of molecules, which is believed to provide further detailed insight into the unique world of quasistructural molecules and the required fingerprints of quasistructural behavior. The quantum statistical mechanics approach seems especially useful and practical when addressing results of novel experimental structure determination techniques, like Coulomb explosion imaging (CEI)[27] and its laser variants.[28,29] Following these comments we return to the traditional picture of "molecular structure" and discuss the related dynamics accessible by spectroscopy at very high resolution.

For the majority of molecules, the energy levels based on the rigid rotor (RR)[30] and harmonic oscillator (HO)[31] approximations to molecular rotations and vibrations, respectively, perhaps after a slight but important extension based on second-order vibrational perturbation theory (VPT2),[32–35] provide a good qualitative and even a semiquantitative understanding of spectral (dynamic) regularities. These molecules are said to be "semirigid" (some call them quasi-rigid) and they do possess a well-defined structure. For semirigid molecules (a) the electronic states are well separated and the one investigated contains a well-defined and conveniently deep (local) minimum, (b) the time and energy scales of the vibrational and rotational motions are

sufficiently different to allow their approximate but meaningful separation, (c) the vibrational eigenstates have well-defined symmetries provided by the point-group symmetry characterizing the unique equilibrium structure of the molecule, (d) the vibrational spacing, defined by small-amplitude vibrations (SAVs), usually starts out large and decreases as the vibrational excitation increases (consider the case of the one-dimensional Morse oscillator,[36] which, by the way, yields the same vibrational eigenspectrum as a quartic oscillator within VPT2), (e) the rovibrational eigenstates can be assigned to a certain vibrational eigenstate (these vibrational eigenstates can be called the vibrational parents[37] of the chosen rovibrational eigenstates), (f) the rotational spectrum provides important and accurate information about the temperature-dependent effective structure[13] of the molecule straightforwardly, and (g) the simple RR picture is perfectly adequate to explain not only the characteristics of the observed microwave (MW) or millimeterwave (MMW) spectra, though hyperfine splitting may also need to be considered, but it is also sufficient to derive the (equilibrium) structure of the molecule via the determination of so-called rotational constants (the lowest-order terms in an effective rotational Hamiltonian[30]). The static and dynamic structures of semirigid molecules are not considered in detail in this review, the interested reader is referred to the large number of excellent textbooks[13,30,31,38–42] available on this topic. Here, we are going to concentrate on molecular systems which are definitely not semirigid and where the RRHO approximation fails to provide a good representation of even the lowest rovibrational eigenstates of the system.

The term "quasimolecule," referring to a molecule having some conjectured characteristics of the static and dynamic structures of a molecule but not all, could be used to name the molecules of interest here. However, this term acquired a special meaning in atomic and molecular physics[43,44] and another meaning in chemistry, in the latter case it refers to molecules stripped of some or most of their electrons (that is, multiply charged cations, existing only under special conditions). These are not the "normal" molecules, straightforwardly amenable to a laboratory investigation, whose unusual structure and internal dynamics we are aiming to describe here. Thus, the term "quasimolecule" is not considered further.

The molecules of interest to this review could also be called fluxional. The term "fluxional molecule" is defined by the Gold Book[12] of IUPAC as follows: fluxional molecules "undergo rapid degenerate rearrangements generally detectable by methods that allow the observation of the behavior of individual nuclei in a rearranged chemical species." This definition puts emphasis on "degenerate rearrangements," which means that the arrangements of the atoms are the same before and after the "chemical event" (like in the cases of degenerate Cope-rearrangement reactions[45,46] and pseudorotation[47]). The original and the rearranged molecules are isoenergetic and can only be distinguished if one numbers the permutationally distinct atoms, as is common practice in the case of the determination of feasible and unfeasible versions of a molecule, when one goes from the complete nuclear permutation inversion (CNPI) group to a molecular symmetry (MS) group during the discussion of the high-resolution rovibrational spectra of molecules.[41,48] Note that for "fluxional molecules" the equilibrium structure does not play the same role as for semirigid molecules, fluxionality is defined with emphasis on nuclear motions. Our claim is that even more unusual molecular structures and rovibrational energy-level patterns can occur if one moves beyond degenerate rearrangements and considers further dynamical movements and processes.

Since the existing usage of the possible terms "quasimolecule" and "fluxional molecule" is not compatible with our task of naming highly unusual structural cases from the point of view of high-resolution spectroscopy, one must invent a new term for molecules which do not have a characteristic equilibrium structure, whose internal nuclear dynamics becomes very complex, and where (some of the) vibrational motions cannot be separated even in zeroth order from the rotations as they have similar energy and time scales. Thus, we introduce the term "quasistructural molecule" for this important and unusual class of molecules.

For a quasistructural molecule, all of the following should hold (to a greater or lesser extent) at the same time: (a) consideration of a single minimum on the PES, even though the molecule may possess only one minimum determinable by methods of electronic-structure theory (this is the case, for example, for the quasistructural H_5^+ and CH_5^+ molecular cations treated in detail below), is insufficient to interpret the structure and the dynamical behavior of the molecule and its observable (high-resolution) spectra, (b) when the structure is averaged, principally over the vibrational ground state(s), it may be significantly (i.e., even qualitatively) different from the equilibrium BO one ("quasistructurality" manifests itself in the effective structure of the molecule, whereby the equilibrium and the ground-state rotational constants may become drastically different), due to strongly anharmonic zero-point motions and the significant occupancy of low-energy (ro)vibrational states, (c) rotational and vibrational spacings are of the same order of magnitude (this is most easily satisfied for light, H-containing molecules) and the internal nuclear dynamics is thus exceedingly complex, (d) spectroscopic characterization of the molecule must rely on MS groups[41,48,49] involving permutation and inversion symmetry operations and feasible and unfeasible motions in the Longuet-Higgins[48] sense, and (e) the set of assigned rovibrational energies of the molecule exhibits unconventional (in the most striking cases "negative") rotational-energy contributions (this is one of the most clear signs of quasistructural

behavior). Note right away that (1) case (b) can happen for molecules considered to be semirigid,[50] and (2) in a few publications[51–56] we called quasistructural molecules "astructural." Nevertheless, we now believe that the new terminology proposed here should replace the old one. A feasible alternative would be to greatly extend the IUPAC definition of "fluxional molecules."

Needless to say, for quasistructural molecules, the observed structures and the rotationally resolved spectra cannot be interpreted using the traditional (RRHO or VPT2) tools of quantum chemistry. Rovibrational Hamiltonians traditionally employed during *variational* nuclear-motion computations and built upon normal coordinates and the Eckart embedding are not suitable for treating quasistructural molecules either. Nevertheless, sophisticated fourth-age[57] variational nuclear-motion computations are able to provide quantitatively correct results, since if the Hamiltonian is expressed in an appropriate set of internal coordinates it is straightforward to define protocols which can handle systems with an arbitrary number of degenerate or nondegenerate minima and arbitrary embeddings can be defined, as well. The accuracy of the results utilizing the best protocols is principally limited by the accuracy of the underlying PES, though the ultimate accuracy limit is the BO separation itself.[58] Interpretation of the complex computed results remains challenging[59] and often there is a clear need for the development of new (ro)vibrational (sometimes rovibronic) models. These models, as far as the vibrations are considered, are different even qualitatively from the conventional HO model.

2 | OF MEASUREMENTS AND COMPUTATIONS

Over the last almost 100 years,[60] natural scientists learned a great deal about how to obtain accurate structures for and interpret sophisticated (gas-phase) high-resolution experimental rovibrational spectra of molecular systems.[42] In the fourth age of research[61] and quantum chemistry[57] we live in, the tools developed by theoreticians allow the quantum-chemical computation of structures as well as spectra with unprecedented accuracy, irrespective how the PES looks like and how many (equivalent or not) minima exist on the PES. This does not mean, however, that the accuracy of even the most sophisticated quantum-chemical computations in predicting rovibrational spectra of polyatomic systems is near that of experiments,[42,62] e.g., those employing frequency-comb techniques,[63–65] but for interpreting complex rovibrational spectra these (variational) quantum-chemical computations often prove to be indispensable.

High-resolution molecular spectroscopy[42] is able to provide extremely accurate and precise energy differences between rovibronic eigenstates (the knowledge and characterization of these eigenstates, providing important information about the dynamics of the system, is extremely important in a large number of scientific and engineering applications[66]). Decades ago, it was hoped that the increased availability of high-resolution experimental data may lead to the development of highly accurate PESs of polyatomic molecules. However, this expectation has not been realized. More than 70 years after the invention of the Rydberg–Klein–Rees technique,[67–69] the model-free inversion of the observed high-resolution spectroscopic data is still constrained basically to the case of diatomic systems.[70] For polyatomic systems one still must use model assumptions of varying sophistication[13] to obtain the dynamic structure of molecules from their observed (high-resolution) spectra.

There has been a steady increase in the number of gas-phase molecules, molecular complexes, and clusters whose internal nuclear motions (rotations and vibrations) are studied at high resolution by ever more advanced techniques of molecular spectroscopy,[42] usually accompanied by ever more sophisticated quantum-chemical (electronic-structure[42,71] and nuclear-motion[42,57]) computations. Quantum-chemical computations are used to aid (or even make possible) the deduction of information encoded in the often exceedingly complex observed spectra.

As a consequence, there is growing evidence that the rovibrational energy-level structure of certain molecular species defies the conceptually simple, traditional interpretation attempts, building upon SAVs and the RRHO approximation. Breakdown of the RRHO approximation means that certain molecular parameters (e.g., the geometric structure[13] and the rotational constants[30]) as well as the rovibrational energy-level structure of these species strongly disagree with the corresponding data computed by (even the most sophisticated) electronic-structure techniques[71] and codes.

The concept of "quasistructural molecules" is also strongly connected to the question when the understanding of the (measurable) rovibrational energy-level structure requires the consideration of the quantum effect of tunneling and when it does not. This issue, arising from point (d) of the definition of quasistructural molecules (*vide supra*), is addressed next. To start, we recall that energy-level splittings, assuming a Coulombic Hamiltonian and no hyperfine interaction terms, are often considered by chemists to be due to tunneling effects. However, this picture is often not correct. Deep tunneling[72–75] is treated as a simple, easily understood and well-utilized concept, in this sense similar to the RRHO approximation. Deep-tunneling regimes, and molecules showing deep tunneling, are not of interest for the present review either. As argued below, when the barriers hindering large-amplitude motions (LAMs) are small, distinguishing tunneling from LAMs may require special

attention. In ambiguous cases, one must consider the effect of isotopic substitution, preferably H/D substitution, as for tunneling cases an increase in the tunneling mass should clearly be seen in the computed, as well as the observed, splittings.

Let us turn our attention to LAMs, as these must characterize quasistructural molecules. Spectroscopists trying to move (much) beyond the RRHO approximation paid particular attention to the development of effective Hamiltonians for molecules with LAMs,[76,77] exemplified by the famous cases of methanol,[78–80] acetaldehyde,[81] and toluene[82,83] (the latter molecule exhibits a diminishing barrier to internal rotation of the methyl group). When LAMs are present, the molecule-fixed axes system tied to the principal axes, a concept working perfectly for semirigid molecules, looses its utility. Thus, different molecule-fixed axis systems have been defined,[81,84–86] providing preferential treatment for different molecules. Interaction of the LAM(s) with the rotational dofs may result in substantial contributions to the energy levels via splittings. One must then emphasize that the rotational energy levels of many molecules exhibiting LAM can be simply described by effective RRHO-based Hamiltonians. The molecules mentioned, even though they do exhibit LAMs, are not quasistructural.

For the particular case of fluxional molecules, it is worth discussing how small or large the barriers need to be in order for the molecule to show fluxional behavior. McKee[87] provides molecular examples for the following types of "fluxionality": (a) valence (e.g., the Cope rearrangement of bullvalene[88]), (b) proton transfer (e.g., malonaldehyde[89]), (c) ring whizzer (e.g., transition metal complexes with cyclic ligands[90]), (d) pseudorotation (e.g., PF_5[91]), and (e) nonclassical bonding (e.g., boranes and carboranes[92]). McKee[87] also points out that core-shell clusters (e.g., gold nanoparticles[93]) and transition-metal complexes (e.g., mixed-valence dinuclear ruthenium complexes[94]) often exhibit fluxional behavior. In Table 1 of Reference 87, McKee presents a summary of the relation between barrier heights and timescales of motions, the interested reader is referred to this table. Note, finally, that for "floppy" van der Waals (vdW) systems, the vibrational motions characterized as LAMs may have a timescale even greater than the rotational timescale. Thus, this appears to be a necessary but not sufficient requirement to classify a molecule as "quasistructural."

A problem experimentalists (in particular, high-resolution spectroscopists) are facing is how to recognize the presence of LAM, fluxionality, and eventually quasistructural behavior in their observed spectra. One must admit that there is no straightforward answer. One problem, explored by Nesbitt[95] for the one-dimensional (1D) "hinge" and "pinwheel" models, is that even for extremely unusual vibrational potentials the rotational-level structure may be fitted well by a rigid or a semirigid effective Hamiltonian. Another example is the alkali trimer Na_3, the textbook example of JT distortion,[19,96,97] whereby the vibrational ground states of both the $\tilde{X}$ and $\tilde{A}$ states can be assigned using a rigid asymmetric rotor,[98] though this approximation breaks down for the lowest $\tilde{A}$-state vibration.[19]

It is naively expected that the concept of a well-defined molecular structure will become ambiguous, or eventually could even break down, if the PES of the molecule possesses several (equivalent or nonequivalent) minima, and the breakdown becomes pronounced once the minima are separated by low barriers (needless to say, "low" depends on the temperature and the experimental technique used for the investigation). Ammonia, NH_3, is an example where two equivalent minima are separated by a relatively low barrier but this does not cause any difficulty with the interpretation of the structure of the molecule.[24] There are only a few real molecules considered where the nuclear motions are governed by slightly nonequivalent minima with low barriers, relevant examples are *meta*-D-phenol[99] and the singly asymmetrically deuterated isotopomer of the vinyl radical, CHD═CH.[100] For molecular systems with several structural isomers, it is customary to treat the low-energy dynamics of each local minimum separately; these systems are again not of interest for the present study.

For vdW complexes of stable (usually semirigid) monomers,[54,101,102] the situation that the low-energy dynamics of the molecule is determined by a large number of degenerate (permutationally invariant) minima, easily accessible with a small amount of excitation energy, can easily occur. The internal dynamics of these molecules, whose monomeric units are held together by secondary (weak) forces, depends not solely on the equilibrium structure(s) but on the placement of several first-, second-, and higher-order transition states, as well as on permutation and inversion symmetry. Treatment of the rovibrational dynamics of these systems is feasible only if one recognizes the need to introduce MS symmetry to the understanding of the characteristics of the measured rovibrational spectra.

Considering the different types of internal motions, it is hard to expect that bond stretching dofs will have a significant role in "quasistructural behavior." On the other end of vibrational softness, torsional and out-of-plane vibrations appear to be the best candidates of the vibrational dofs which could couple extremely strongly with the rotational dofs.

The unusual rovibrational energy-level structure of quasistructural molecules calls for unusual modeling efforts to interpret relevant observations and/or computations. Successful modeling efforts have been made for fluxional molecules and beyond,[52,56,95,103,104] and some, like the cases of (nearly) free (torsional) motion[103] and vibrational quantum-graph theory,[56] will be discussed in later sections of this review. Before that, however, we are going to discuss a couple of cases where some

important aspects of quasistructural behavior are satisfied but when the molecular system should still not be considered quasistructural.

3 | ON THE SEPARATION OF VIBRATIONS AND ROTATIONS

There are certain floppy molecular systems where the timescale of at least one large-amplitude vibrational motion is comparable to the timescale of the rotations. It is this aspect of quasistructurality which is relevant for the discussion of this section. In such cases one can still rely on an approximate adiabatic separation of fast and slow motions but the dynamics of the large-amplitude vibration must be treated together with the rotations.

3.1 | Pseudorotation

The concept of pseudorotation, the "mutation" of a vibrational dof into a rotational dof, was introduced by Kilpatrick et al.[47] to explain abnormal entropy and heat capacity values[105,106] observed for gaseous cyclopentane. Pitzer and coworkers argued that one of the two lowest-frequency degenerate (assuming D_{5h} point-group symmetry for the structure) ring-puckering modes of cyclopentane mutates and shows the properties of a rotation (basically no hindering potential). Pseudorotation[107] is a special form of large-amplitude nuclear motions, distinctively different from SAVs about a single equilibrium structure. Pseudorotation involves several isoenergetic, permutationally distinct "equilibrium" structures separated by exceedingly small barriers (which can even be neglected for a qualitative understanding of the motion). As a consequence, molecules for which pseudorotation has been established do not possess a static molecular structure but the structures are determined by dynamic effects, which is another characteristic of quasistructural molecular systems. Converting the puckering/twisting model Hamiltonian corresponding to the Pitzer model to polar coordinates[108] enables the clear visualization of the pseudorotation of cyclopentane[109]: interconversion of the 10 energetically equivalent but permutationally distinct twist minima (of C_2 point-group symmetry) through 10 bent conformations (of C_s point-group symmetry), with diminishing barriers. Thus, while the equilibrium structure of cyclopentane is a polar asymmetric top, the "true" structure of the molecule becomes a nonpolar symmetric top.[107,109] In the case of cyclopentane, pseudorotation is fast on the timescale of the "external" rotations. This means that high-resolution spectra of cyclopentane[110] can be interpreted based on traditional Hamiltonians, perhaps of a slightly awkward form. All this means that cyclopentane is *not* a quasistructural molecule, just a fluxional one.

Another case of pseudorotation relevant for the present discussion is a rotating molecule trapped in a cage (e.g., CO in solid Ar matrix[111]). In such host–guest systems, the atoms of the solid matrix follow the rotation of the guest molecule and perform what can be called synchronous pseudorotation. Allowing for the nonrigidity of the lattice, not considered in the Devonshire cell model,[112] introduces two effects changing the quantum treatment of these systems: (a) the host–guest (molecule–crystal) interaction energy is minimized by the relaxation of the lattice, and (b) the orientation-dependent lattice relaxations, through coupling of the guest rotations with pseudorotation of the host, induce a significant change, in fact a decrease of the effective rotational constants. Recently, quantum studies[113] of molecules trapped in cages[113,114] found renewed interest, especially with regard to the joint treatment of translation–rotation states. Answering the question whether these systems are quasistructural or not would require detailed experimental high-resolution spectroscopic studies and variational rovibrational treatments, both hindered by the size of some of these systems.

A further important class of molecular systems where inclusion of pseudorotation plays an important role when explaining spectral features is formed by molecules exhibiting JT[18] distortion. For example, a combined treatment of rotation and pseudorotation has been used to interpret high-resolution spectra of the ground states of Li_3 and Na_3.[19] Furthermore, Merkt and coworkers[21,115–117] studied the LAMs and the rovibronic energy-level structure of the methane cation, CH_4^+, and several of its deuterated isotopologues. Since the Li_3, Na_3, and CH_4^+ species are open-shell molecules and the present review deals with closed-shell molecules, the discussion of these JT-distorted cases, calling for a joint treatment of rotation and pseudorotation, is not pursued here.

3.2 | Semirigid benders

An early example of joint rotation–vibration treatments beyond the RRHO model is the "semirigid bender" analysis method developed by Bunker and coworkers.[118,119] This technique proved to be crucial for the proper treatment of the high-resolution spectroscopy of triplet methylene.[120] While singlet methylene is a semirigid molecule, triplet methylene is a "floppy" system. The PES of triplet methylene ($^3CH_2$ in our shorthand notation) is rather shallow along the bending mode, with a barrier to

linearity less than 2,000 cm^{-1}. While this caused some problems for some of the earlier computations (see Reference 121 for details), the rotational transitions on the (0 0 0) vibrational ground state appear to be perfectly regular and the comparison of the computed results[121] with the experimental ones[122] shows the behavior expected for a semirigid molecule.

Note that CH_2 played a unique role in the development of modern quantum chemistry, it has become a "paradigm for quantitative quantum chemistry."[123] Theory proved experiment[124] wrong both about the structure of CH_2 (linear vs. bent) as well as the singlet-triplet energy separation (small vs. large).[125–127] As it turns out from the full-dimensional variational treatment of the vibrations and rotations of $^3CH_2$,[121] it is indeed somewhat challenging to obtain the rovibrational states of this "floppy" species but it is not a quasistructural molecule.

The nuclear motions of the *quasilinear* molecules carbon suboxide, C_3O_2,[128,129] and HCNO[119] provide other typical examples where the semirigid-bender treatment can successfully interpret results of high-resolution spectroscopic measurements. While for the semirigid bender molecules mentioned treatment of one vibrational dof together with the rotational dofs is necessary, several other criteria for classifying these molecules as quasistructural ones are not satisfied.

4 | ON UNUSUAL EFFECTIVE ROTATIONAL CONSTANTS

As stated in Section 1, quasistructural molecules are characterized by highly unusual rotational constants, reflecting the substantial differences between the static equilibrium and the dynamic effective structures of these species. Nevertheless, not all systems exhibiting unusual rotational constants belong to the class of quasistructural molecules. Some relevant nonquasistructural examples are provided in this section, while, for example, the quasistructural halogen-bonded complexes,[130–135] characterized by effective rotational constants which may deviate by up to an order of magnitude from their equilibrium counterparts, will be discussed later.

4.1 | Rotation-internal-rotation (RIR) theory

A number of molecular systems exhibiting internal rotation motion (like that of the methyl or NO_2 groups) can be modeled by building on the concept of molecular fragments. The structure of the molecular systems under discussion is assumed to have a "top" and a "frame" moving with respect to each other. One can choose both the top and the frame as firmly rigid entities[136] but one can also relax their structure as the top rotates with respect to the frame, yielding semirigid models. These types of semirigid models were pioneered by Günthard and coworkers.[137]

To move forward, let us take nitrobenzene as an example. As shown by Günthard and coworkers,[137] to reproduce the experimental effective rotational constants of nitrobenzene better, it is necessary to relax the rigidity of the top (in the particular case of nitrobenzene the ONO angle). While relaxation of the top (or the frame) helps obtaining better agreement between modeling attempts and experimental rotational constants, the improvement can be considered minor and even the rigid models usually ensure satisfactory, semiquantitative agreement. Systems which need to be treated by RIR theory show that the distorted spinning top gives rotational constants (slightly) different from the equilibrium ones. These small changes are certainly both important and highly relevant but they do not make the molecules treatable via RIR theory members of the family of quasistructural molecules.

4.2 | Host–guest systems

Pseudorotation of the cage surrounding a guest molecule, a case which has importance also for matrix isolation spectroscopy, was discussed in Section 3.1. As noted there, such host–guest systems may exhibit somewhat "strange" rotational constants, deviating substantially from their equilibrium counterparts. However, due to the lack of relevant experimental or theoretical high-resolution data this case is not discussed further. It is only stated here that certain host–guest systems may show quasistructural behavior but certainly not the majority of such systems.

5 | ON REARRANGEMENT REACTIONS

In organic chemistry there are several so-called rearrangement reactions which heavily involve spatially constrained nuclear motions and thus are of interest for this review. These rearrangement reactions include the Cope,[45,46,138,139] the aromatic and aliphatic Claisen,[140,141] the Bergman,[142] and the Myers–Saito[143] reactions.

The most basic structural requirement of the Cope rearrangement is the presence of two π bonds in the 1 and 5 positions in a carbon chain. Thus, the archetype of the degenerate Cope rearrangement is 1,5-hexadiene. Both the Cope and the Claisen rearrangements are $[3_s,3_s]$ sigmatropic shift processes. Furthermore, from the structural point of view, the Bergman[142] and the Myers–Saito[143] reactions can also be considered as members of the extended Cope rearrangement family with two branches, 6π and $[2\sigma + 4\pi]$.[139]

Bullvalene, $C_{10}H_{10}$, also known as tricyclo[3.3.2.0]deca-3,6,9-triene, is a member of the family of $(CH)_n$ molecules, with smaller members including benzene, C_6H_6, and cyclooctatetraene, C_8H_8. To reconcile the chemical properties of the $n = 6$ and 8 molecules with their structure, it is widely accepted to consider benzene as an "aromatic" molecule, while cyclooctatetraene as a nonaromatic polyene. Based on proton nuclear magnetic resonance (NMR) measurements,[46] bullvalene is usually described[46,88] as "structureless" and highly "fluxional," a "molecule that has no permanent structure"[88] and thus no permanent carbon–carbon bonds. The small cage-like bullvalene molecule is characterized by physical organic chemists as a molecule capable of undergoing spontaneous Cope rearrangement, interconverting a huge number of degenerate "isomers." As argued by Doering and Roth,[46] the fact that the 10 carbon atoms and the 10 protons of bullvalene are chemically equivalent (^{13}C and ^1H NMR spectra show a single line at elevated temperature) means that "all ten carbon atoms inevitably wander over the surfaces of a sphere in ever changing relationship to each other."[46]

We are not aware of rotationally resolved high-resolution spectroscopic studies on bullvalene; thus, one can only speculate whether this "fluxional" molecule is also "quasistructural" or not. At present we tend to think that this molecule is not quasistructural. In fact, the infrared (IR) spectrum, unlike the NMR spectra, of bullvalene[46] does not vary with change in the temperature. This experimental finding can be rationalized by noting that IR spectroscopy is orders of magnitude faster than NMR spectroscopy.

The Cope rearrangement of 1,5-dimethyl-semibullvalene-2(4)-d_1[144,145] is one of the prime examples of heavy-atom tunneling,[74,75] in this case carbon tunneling,[75] a quantum effect of high interest for the present review. Often via highly innovative experimental schemes, carbon tunneling has been shown to take place in a number of further small chemical systems, including the automerization of cyclobutadiene,[146,147] the ring opening of a strained cyclopropene to a triplet carbene,[148] and the low-temperature ring expansions of a fluorocarbene, containing a four-membered ring, to a fluoro-cyclopentene[149] and of a benzazirine, containing a six-membered ring, to a seven-membered keteneimine heterocycle.[150] All these cases prove beyond reasonable doubt that heavy-atom tunneling is a quantum phenomenon which organic chemists may need to consider when dealing with certain reaction systems. Unfortunately, no high-resolution spectroscopic data are available for the systems mentioned. Thus, it is not clear whether quasistructurality plays a role in the nuclear dynamics of these tunneling systems or not. Perhaps the most interesting and most straightforward investigation would be the study of the high-resolution spectroscopic consequences of the automerization (isomerization) reaction of cyclobutadiene-1,4-d_2 to cyclobutadiene-1,2-d_2, where the measurement temperatures were between −50 and −10°C and the claim is that close to 100% of the isomerization reaction proceeds via tunneling.[75,146,147,151]

6 | EXAMPLES OF QUASISTRUCTURAL MOLECULES

6.1 | H_5^+ and its deuterated isotopomers

As predicted by all sophisticated electronic-structure computations, the equilibrium structure of the H_5^+ ion resembles that of a solvated ion, with the core H_3^+ ion, formed by a strong 3-center–2-electron (3c–2e) bond, solvated by a H_2 molecule, placed perpendicularly to the H_3^+ plane. The height of the torsional barrier, hindering the internal turnaround of the seemingly loosely attached H_2 subunit, is rather low, $\sim 80\,cm^{-1}$.[51–53]

The H_5^+ ion lacks the usual (heavier) central atom that may form multiple strong (covalent, often 2c–2e) bonds, typical for virtually all small molecular species. As a result, the static asymmetric C_{2v} equilibrium structure of H_5^+ is not the effective structure of the cation. In particular, on the vibrationally averaged PES the $\sim 60\,cm^{-1}$ electronic barrier, hindering the proton hopping motion between the two sides, disappears, resulting in no difference in the "left" and "right" H_2 units for $H_5^+ \equiv [H_2–H–H_2]^+$. Unlike in the case of semirigid molecules, the lack of a clear structure makes the rovibrational energy-level set of H_5^+ challenging to anticipate as well as to interpret.[51–53,152–168]

While the variational-like computation of the large number of *vibrational* eigenstates of H_5^+ was only technically difficult,[53,159,160,163] interpretation of the *rovibrational* eigenstates of H_5^+ proved to be a real challenge.[51] Assigning rigid-rotor labels and vibrational parent states[37] to rovibrational eigenstates of H_5^+ revealed a very different behavior from the RRHO model: extreme mixing of the vibrational parent states.[51]

The unusual dynamical features place H_5^+ into the family of quasistructural molecules. The complex dynamics occurs partly due to the coupling of the (nearly free) torsional vibration with one of the rotational dofs, that corresponding to the

torsional axis. Since the torsional motion is the lowest-energy vibration of H_5^+, this effect determines the whole set of computed eigenenergies. The rovibrational eigenstates having no torsional excitation can be explained using effective rotational constants whereby A is twice as large as its equilibrium value.[51] To explain levels with torsional excitations, apart from doubling of the A rotational constant, explicit consideration of the torsion–rotation coupling is also necessary.[51]

The peculiar rovibrational energy-level structure of H_5^+ can be reproduced surprisingly well in a four-dimensional (4D) model considering only the torsional vibration and the three rotational dofs.[51,52] This model is described in detail in Appendices A and B to this paper. A brief summary of the derivations and results provided in Appendix B for H_5^+ and D_5^+ is as follows: (a) a torsion–rotation model with two parameters and zero torsional potential is able to accurately reproduce most of the torsion–rotation energy levels, (b) in some cases significant deviations from the energy levels predicted by the zero-potential torsion–rotation model are observed; these deviations always go hand in hand with energy-level splittings which can be accounted for by a first-order perturbative treatment of the torsional potential, and (c) these splittings are attributed to the weak torsional potential treated as a perturbation and not to tunneling between the two equivalent torsional potential wells. The last conclusion is also supported by the observation that the splittings are virtually insensitive to deuteration.[53] The very unusual dynamical behavior of H_5^+ holds true for all D-substituted isotopomers and isotopologues,[53] strongly suggesting that this unusual behavior is connected to the shape of the PES and not to the fivefold permutation symmetry of the H_5^+ and D_5^+ molecules.

6.2 | CH_5^+ and the vibrational quantum-graph model

Perhaps the most striking example of quasistructurality is provided by protonated methane, CH_5^+, the prototype of penta-(or higher-)coordinated "nonclassical" carbocations showing rich and exotic chemistry.[169] CH_5^+, owing to its peculiar rovibrational quantum dynamics and highly complex and congested infrared spectra even at very low temperatures, has puzzled the community of high-resolution molecular spectroscopists for more than two decades.[170–175] Finally, experiments redefining the state-of-the-art have led to the determination of a large number of energy combination differences, yielding some of the lowest rovibrational energy levels of CH_5^+.[174,175]

Electronic-structure studies revealed that the equilibrium structure of CH_5^+ has C_s point-group symmetry and that it can be characterized as a H_2 moiety attached to a strongly bound CH_3^+ unit (a tripod).[176,177] Based especially on the congestion and complexity of the low-temperature infrared spectra, it was also concluded that the barriers hindering the complete scrambling of the five protons are essentially zero, implying that CH_5^+ is a "highly fluxional molecule without a definite structure."[177] The $5! = 120$ permutationally related, "equivalent" equilibrium structures (versions) can be interconverted by clockwise and counterclockwise internal rotations of the H_2 unit by 60°, and by the so-called flip motion that exchanges a pair of protons between the CH_3^+ and H_2 units.[178] The electronic barriers hindering the internal rotation and flip motions are only about 30 and 300 cm^{-1}, respectively, allowing facile exchange of the protons; therefore, the internal dynamics of CH_5^+ must be described by the MS group S_5^* (or G_{240}).[41] The number of versions can be expressed as the quotient of the order of the MS group and that of the point group, encompassing the geometrical symmetries of a selected version. This general and elegant group-theoretical method to determine the number of versions[55,179,180] relies on Lagrange's theorem[181] and yields $|S_5^*|/|C_s| = 240/2 = 120$ versions for CH_5^+.

The development of accurate potential energy and electric dipole moment hypersurfaces[182,183] for CH_5^+ allowed the quantum-chemical characterization of the rovibrational dynamics of CH_5^+. Earlier studies[178,184–195] yielded rovibrational energy-level patterns that even qualitatively differ from the results of variational nuclear-motion computations.[55,196–198] The variational results also revealed that the rovibrational energy-level pattern of CH_5^+ defies any interpretation attempts based on the standard RRHO model. Moreover, group-theoretical studies found that in CH_5^+, in contrast to the majority of molecules, it is virtually impossible to separate the vibrational and rotational dof.[197,199]

In References 55 and 56, it was concluded that models based on tunneling between the 120 equivalent potential wells fail to account for the rovibrational energy-level pattern of CH_5^+. Nevertheless, the low rotation and flip barriers do not imply that the protons can move freely, as their motion is strongly correlated. Based on these arguments the low-energy quantum dynamics of CH_5^+ is perhaps best described by a model based on the concept of *quasi-free motion*,[55,56] and consideration of the internal rotation and flip motions is necessary and at the same time seemingly sufficient for understanding the low-energy quantum dynamics of CH_5^+.

The unusual vibrational quantum dynamics of CH_5^+, the topology of the CH_5^+ PES, and the concept of quasi-free motion inspired the introduction of the simple and intuitive vibrational quantum-graph model.[56] Although the quantum-graph

model[200,201] has been applied in electronic structure theory[202–205] and in various fields of physics,[206–211] it had not been employed to treat nuclear motions before 2018.[56] The vertices of the vibrational quantum graph (Figure 1) represent versions of the equilibrium structure with distinct atom numbering, while the edges refer to collective nuclear motions transforming the versions into one another. These definitions allow the mapping of the complex vibrational quantum dynamics of CH_5^+ onto the motion of a particle confined in a quantum graph. Since it is expected that this approach will find application in describing quasi-free motion in the future treatment of quasistructural molecules, the most important characteristics of the technique are given here.

In order to construct the Schrödinger equation for a particle moving along the edges of the quantum graph, it is necessary to postulate that each edge possesses a length (the vibrational quantum graph is a metric graph). The Hamiltonian expressed in atomic units has the simple form

$$\hat{H} = -\frac{1}{2}\frac{d^2}{dx^2} + V(x) \tag{1}$$

where $x \in [0, L_j]$ is a mass-scaled local coordinate defined along the jth edge of length L_j. As the barriers hindering the internal rotation and flip motions of CH_5^+ are low, the discussion can be safely limited to the case of free motion ($V(x) = 0$). Then the eigenfunctions of $\hat{H}$ along the jth edge are superpositions of outgoing and incoming plane waves,

$$\psi_j(x) = a_j \exp(\mathrm{i}kx) + b_j \exp(-\mathrm{i}kx) \tag{2}$$

with the corresponding energy eigenvalues $E_k = k^2/2$. The energy levels are quantized by the Neumann boundary conditions[200,201] expressing the continuity of the wave function and the conservation of the quantum flux.

Figure 1 shows the structure of the quantum graph of CH_5^+, the 120 equivalent vertices are connected by 120 internal rotation and 60 flip edges. Due to the high symmetry, the quantum graph of CH_5^+ can be parameterized with just two different

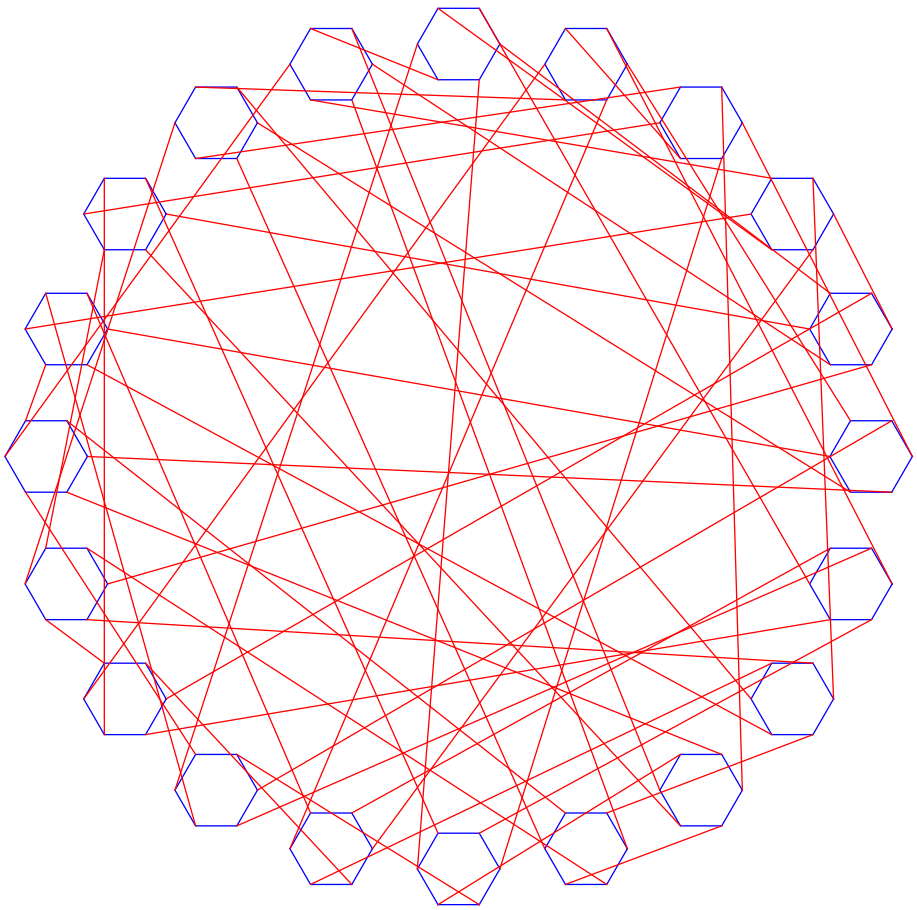

FIGURE 1 Pictorial representation of the quantum graph applied to the quantum-dynamical description of the low-energy vibrations of CH_5^+. The 120 internal rotation and 60 flip edges connecting the 120 equivalent vertices (versions) are indicated by blue and red lines, respectively

TABLE 1 Low-lying vibrational energy levels (in cm^{-1}, the zero-point energy is set to zero) of CH_5^+ and CD_5^+ with S_5^* symmetry labels (Γ). The seven-dimensional (7D) constrained, bend-only variational vibrational energy levels (VAR) are compared to their counterparts obtained by the quantum-graph model (QG)

CH_5^+			CD_5^+		
Γ	VAR	QG	Γ	VAR	QG
A_1^+	0.0	0.0	A_1^+	0.0	0.0
G_2^-	9.8	11.4	G_2^-	4.1	4.6
H_1^+	20.3	22.2	H_1^+	10.0	8.9
H_2^-	41.1	39.6	H_2^-	17.4	15.9
G_1^+	49.3	44.8	G_1^+	18.7	18.1
I^-	58.2	49.7	I^-	21.8	20.1
H_2^+	59.1	50.2	H_2^+	23.0	20.2
I^+	111.4	95.2	I^+	40.5	38.4
G_2^-	112.3	100.9	G_2^-	40.8	40.8
H_1^-	113.4	96.0	H_1^-	41.6	38.6
H_1^+	121.3	112.4	H_1^+	47.4	45.2
H_2^-	139.1	148.7	H_2^-	59.4	59.8
G_1^+	154.2	182.0	G_1^+	67.7	73.3
A_2^-	197.8	284.5	A_2^-	84.2	114.5

edge lengths, L_1 and L_2, corresponding to the internal rotation and flip edges, respectively. Following the considerations of Reference 56, the numerical edge length values $L_1 = 61.2\sqrt{m_e}a_0$ and $L_2 = 1.0\sqrt{m_e}a_0$ (CH_5^+) and $L_1 = 96.7\sqrt{m_e}a_0$ and $L_2 = 1.1\sqrt{m_e}a_0$ (CD_5^+) can be used to compute the quantum graph's vibrational energy levels.

Table 1 compares the quantum graph's vibrational energy levels to their counterparts (seven-dimensional [7D] bend model) computed by variational nuclear-motion codes.[55,56,196,198] The results presented in Table 1 show that the simple quantum-graph model is able to reproduce the lowest variational vibrational energy levels of CH_5^+ and CD_5^+ remarkably well. Even though the particle can move freely along the edges of the quantum graph, the important features of the PES of CH_5^+ are implicitly taken into account in the quantum-graph model as the connectivity is determined by the shape of the PES. Another related and promising approach to interpret the rovibrational energy-level pattern of the quasistructural CH_5^+ molecule is the recently developed five-dimensional rigid-rotor model.[212–214]

6.3 | $C_2H_3^+$

Electronic structure computations predict[215] that protonated acetylene, $C_2H_3^+$, has a "nonclassical," planar "bridged" equilibrium structure with a 3c–2e bond formed by one of the Hs (the "proton") of the cation and the two C atoms, whereas the other two Hs point very slightly toward the bridging proton. The $C_2H_3^+$ ion has a low-energy structural isomer characterized by a Y shape, with a relative energy of +5 kcal mol^{-1}.

The structure of protonated acetylene has been investigated in Coulomb-explosion imaging (CEI)[27] experiments. The CEI studies[216,217] on $C_2H_3^+$ clearly suggested that the most probable effective, "experimental" structure of the cation is very different from the computed equilibrium one: $C_2H_3^+$ has a strongly nonplanar structure due to LAMs of the hydrogens, especially that of the bridging one.

Marx et al.[218] simulated and interpreted the results of the CEI experiments via computing the many-body nuclear-density distribution function, the diagonal part of the many-body nuclear-density matrix. The simulations employed both the standard Car–Parrinello ab initio molecular-dynamics method[219] and its quantum variant, the path integral technique.[220] A detailed, reduced-dimensional analysis, employing the five internal angular coordinates and permutational symmetry coordinates of the three polar angles, suggested a strong (30°) deviation from linearity for the acetylene backbone, resulting in a *trans*-bent form. Furthermore, the bridging proton forms a ring around the middle point of the CC bond, perpendicular to the main symmetry axis. Thus, the effective and the equilibrium structures of $C_2H_3^+$ are drastically different, as expected for a quasistructural molecule.

While to the best of the authors' knowledge no high-resolution spectroscopic data are available for $C_2H_3^+$, it appears safe to conjecture that this molecule is indeed quasistructural. In fact, due to the highly mobile nature of the proton it is expected that

most protonated simple closed-shell molecules would show complex nuclear dynamics,[221] similar to that observed for protonated CH_4 and C_2H_2. Most likely, the cations of a number of closed-shell species would be characterized as quasistructural.

Perhaps even more interesting would be to obtain experimental high-resolution spectroscopic data for doubly protonated species, such as CH_6^{2+}. Interpretation of the experimental results, if they could be obtained, would be especially challenging but also especially rewarding if certain models were able to capture the essence of the complex nuclear dynamics of these cations.

6.4 | Halogen-bonded complexes

One of the characteristics of quasistructural behavior is the substantial difference between the equilibrium and the effective structures of the molecule. This difference means that the measured effective rotational constants will differ significantly, way beyond what VPT2 theory predicts[34,35] for semirigid molecules, from the rotational constants belonging to the static equilibrium structure. There are a couple of cases known to the authors, they are all halogen-bonded complexes, where *substantial* differences in equilibrium versus effective rotational constants has indeed been observed.

Over a larger period of time, Caminati and coworkers published a considerable number of studies in which the rotational spectra of several complexes held together by halogen bonds (HaBs) have been investigated. The HaB complexes investigated and relevant for this review include $CF_4{\cdot}H_2O$,[130] $CF_3Cl{\cdot}H_2O$,[131] $CF_3Cl{\cdot}NH_3$,[132] CF_4·pyridine,[133] $CF_3Cl{\cdot}CH_3F$,[134] and CF_3Cl·dimethyl ether,[135] with the common theme that one of the rotational constants (A in all cases) fitted to the experimentally measured pure rotational transitions is hugely different (up to an order of magnitude[134]) from the one corresponding to the static equilibrium structure computed via electronic-structure theory. There is a straightforward explanation of the overly large effective A rotational constant, offered by Caminati et al.[130–135]: the coupling of (an almost) free internal rotation with one of the rotational dofs, corresponding to the axis closest to the free internal rotation axis of one of the monomer (e.g., CF_3Cl) units (see Appendix A of this review). To the best of our knowledge, no rovibrational spectroscopic studies have been performed for these molecular complexes; thus, we do not know whether the rovibrational states would show quasistructural behavior. Nevertheless, both the experimental (Fourier transform microwave [FTMW] spectroscopy) observations and the explanation of the experimental peculiarities observed make us speculate that these complexes may belong to the family of quasistructural molecules.

There are further experimental peculiarities of these complexes; for example, instead of being an asymmetric top, the effective structure of $CF_4{\cdot}H_2O$, as observed experimentally, is that of a symmetric top. In summary, all these molecular complexes held together by HaB exhibit behavior which makes them candidates of the family of quasistructural molecules.

6.5 | $CH_4{\cdot}H_2O$ and its deuterated isotopomers

Two and a half decades ago, detailed far-infrared (FIR) spectroscopic measurements were carried out for the $CH_4{\cdot}H_2O$ dimer in the laboratory of Saykally.[222] A substantial number of the observed transitions could not be assigned due to the complexity of the spectrum. Eventually, variational computation[54,104] of the rovibrational eigenstates of $CH_4{\cdot}H_2O$, within the rigid-monomer approximation leaving only the six intermonomer coordinates active for the treatment of the low-energy dynamics, and the unambiguous assignment[54] of the eigenstates of the six-dimensional (6D) model system yielded an explanation of the spectrum and clear signs of peculiar nuclear quantum dynamics for this dimer. The computations occasionally found reversed ordering of the vibrational and rovibrational levels, ultimately resulting in negative rotational energy increments. The computational results[54] thus provide strong evidence of quasistructural behavior for this complex.

The equilibrium structure of the $CH_4{\cdot}H_2O$ dimer has a low, C_s point-group symmetry, allowing vibrations of A′ and A″ symmetry. However, the low-energy vibrational-level structure of the $CH_4{\cdot}H_2O$ dimer can only be understood if one introduces the considerably more complex MS symmetry into the dynamical treatment. The MS group describing the internal motions of $CH_4{\cdot}H_2O$ is G_{48}.[41,54,104] As a result of the interaction of the $|G_{48}|/|C_s| = 24$ allowed versions of the dimer, the representations generated by 24 vibrational states of either A′ or A″ symmetry split into the direct sum of the following one-, two-, and three-dimensional irreducible representations[54]:

$$\Gamma_{\text{dimer}}(\text{A}') = \text{A}_1^+ \oplus \text{E}^+ \oplus \text{F}_1^+ \oplus 2\text{F}_2^+ \oplus \text{A}_2^- \oplus \text{E}^- \oplus 2\text{F}_1^- \oplus \text{F}_2^- \tag{3}$$

$$\Gamma_{\text{dimer}}(\text{A}'') = \text{A}_2^+ \oplus \text{E}^+ \oplus 2\text{F}_1^+ \oplus \text{F}_2^+ \oplus \text{A}_1^- \oplus \text{E}^- \oplus \text{F}_1^- \oplus 2\text{F}_2^- \tag{4}$$

The variationally computed rovibrational eigenstates[54,104] reveal that the measured FIR transitions are not associated with different vibrationally excited states in the traditional sense, but with rovibrational transitions between the different rotationally excited states of the heavily split ground vibrational state manifold of the dimer (see Equations (3) and (4)). The measured[222] and computed[54] rovibrational transitions are in excellent agreement, providing experimental support for the computed negative rotational-energy contributions.

The peculiar characteristics of the rovibrational eigenstates computed can be explained[104] if the overall internal rotations of the complex are modeled as rotations of two coupled, rotating (rigid) monomers. The coupled-rotor (CR) model[104] explains that for a given total rotational quantum number, J, the negative rotational excitation energies correspond to the rotational de-excitation of one of the monomers (in the methane-water case, that of water), while at the same time, the rotational excitation of the other monomer and of the diatom increases, all governed by the internal couplings of the monomer and diatom rotations.

Very similar rovibrational features were computed[104] for the deuterated isotopomers of the methane–water dimer. For them, however, there is a lack of supporting experimental information. Nevertheless, it is clear that these molecules are also quasistructural. The CR model not only assists our understanding of the quasistructurality present in the $CH_4{\cdot}H_2O$ system, but it also provides arguments for the joint treatment of the vibrational and rotational motions in the case of loosely bound clusters.

In summary, the methane–water dimer, $CH_4{\cdot}H_2O$, is a loosely bound vdW complex, for which clear experimental spectroscopic evidence of quasistructurality is available. The dimer displays all the characteristic features of quasistructurality: the vibrational ($J = 0$) energy-level structure can only be understood if the concept of MS symmetry is introduced into the dynamical treatment, the effective structure of the dimer, besides accepting the rigidity of the monomer units, is heavily influenced by the vibrational dynamics, and the complex shows negative rotational excitations. It is expected[102] that the methane–methane dimer, with an MS symmetry of G_{576} and $|G_{576}|/|D_{3d}| = 576/12 = 48$ allowed versions, exhibits even more clear signs of quasistructurality, but this needs experimental verification.

6.6 | Dimethylacetylene

Dimethylacetylene, $CH_3{-}C{\equiv}C{-}CH_3$, contains a linear carbon chain and two coaxial methyl rotors. Dimethylacetylene has one LAM: internal rotation of one methyl group with respect to the other, with a very small torsional barrier height, about 6 cm^{-1}, hindering this motion.[223] For dimethylacetylene, one of the rotational axes coincides with the two methyl internal rotor axes, resulting in the nonseparability of the two internal-motion types. Thus, one of the important criteria of quasistructural behavior is clearly fulfilled. It is also worth mentioning that (a) the anomalous specific heat capacity of dimethylacetylene[224,225] has been explained[225] by free internal rotation and (b) understanding the measured spectra with even extended effective Hamiltonians proved to be extremely difficult if not impossible.[223,226,227]

To describe the internal motions of dimethylacetylene, one needs the G_{36} MS group.[41,49] Since the equilibrium structure of dimethylacetylene has D_{3h} point-group symmetry, understanding the dynamics of the molecule requires the consideration of $|G_{36}|/|D_{3h}| = 36/12 = 3$ versions of the molecule. This means that another criterion of quasistructural behavior is fulfilled for dimethylacetylene.

Figure 4 of Reference 52 reported the correlation between the reduced energies and the reduced barriers of a two-dimensional vibration–rotation model developed to explain the peculiar rovibrational energy-level structure of H_5^+.[51] The one-dimensional vibrational (along the torsional dof, φ) part of the model Hamiltonian is

$$\hat{H}^{1D} = -2\beta\frac{\partial^2}{\partial\varphi^2} + \hat{V}(\varphi) \tag{5}$$

and the potential curve, for H_5^+, is approximated as

$$\hat{V}^{1D}(\varphi) = \frac{V_0}{2}[\cos(2\varphi) + 1] + V_{min} \tag{6}$$

The reduced barrier corresponding to this model is defined as $v_0 = V_0/\beta$, while the reduced energies are $\epsilon^{2D} = E^{2D}/\beta$. For small v_0 values, one is close to the zero-barrier limit, while for large v_0 values, one is approaching the semirigid-molecule limit (see Appendices A and B). As expected, the two limits can be described by two sets of quantum numbers.[52]

It is thus of considerable interest to report v_0 values for a couple of molecules treated by high-resolution spectroscopy. For the molecules dimethylacetylene, H_5^+, methanol, ethane, and diphenylacetylene, the v_0 values are 1.1, 1.5, 44, 188, and 533, in order. The transition from free to semirigid behavior happens at about $v_0 = 30$. The first important conclusion one can draw from these numbers is that dimethylacetylene is clearly a quasistructural molecule. The second conclusion is that the rovibrational energy-level structure of ethane, methanol, and diphenylacetylene is clearly that of a semirigid molecule (note especially the drastic difference between the dynamical behavior of dimethylacetylene and diphenylacetylene). Furthermore, as noted by Bunker and Jensen,[41] "except in ultrahigh resolution spectroscopic studies ethane can be considered to be a rigid molecule and the possibility of torsional tunneling can be neglected." Finally, the peculiar and heavily split energy-level structure characterizing the low reduced-barrier limit can be deduced from Figure 4 of Reference 52. Once again, the splittings at the low reduced-barrier limit are not due to tunneling but to the perturbative effect of the weak potential on the energies corresponding to the free limit.

In summary, despite the lack of relevant experimental and computed data, it can be safely stated that dimethylacetylene provides one of the prime examples of molecules exhibiting quasistructural behavior.

7 | SUMMARY AND CONCLUSIONS

The classical-mechanics-based model of associating a static structure to quantum systems called molecules is rooted deeply in the minds of practitioners of chemistry, physics and molecular biology, as this simple model successfully explains a large number of phenomena of interest to them. Furthermore, this static picture forms the basis of the simplest dynamical picture of molecular (nuclear) motions: rigid rotations and SAVs about a well-defined (minimum-energy) structure. Nevertheless, as the resolution and the accuracy of the traditional experimental techniques probing molecular structures and spectra in the gas phase improved and more and more new, sophisticated high-resolution spectroscopic techniques have become available, more and more molecular systems have been discovered where this picture does not hold and where assuming a single structure, corresponding to a minimum on the clamped-nuclei PES computed by means of standard electronic-structure theory, does not provide a good representation of the spectral features observable under high resolution.

Clearly, neglect of nuclear dynamics when determining the structure of the molecule has only minor, purely quantitative consequences for the majority of the molecules investigated in the gas phase. When this is true, the molecule is called semirigid. However, there is a growing class of molecules whose effective structures cannot be understood without the explicit consideration of slow nuclear motions (rotations and large-amplitude vibrations). These molecules are often called floppy, flexible, or fluxional. This review focuses on a new class of molecular systems where complex internal motions have even more dire consequences on the structure and spectra than established for flexible molecular systems and where permutation-inversion symmetry of the system cannot be neglected during the study of the dynamics. These are what we call quasistructural molecules.

For quasistructural molecules, all of the following should hold simultaneously: (a) the notion of a static structure, usually called an "equilibrium structure," corresponding to a minimum on the PES of the molecule, looses its strict meaning and fails to represent the effective structure of the molecule, (b) internal nuclear motions (rotations and vibrations, translation can be separated for all but certain confined systems) become dominant, resulting in effective molecular structures often even qualitatively different from the equilibrium ones, (c) separation of the internal nuclear motions breaks down almost completely, rotational and vibrational dof cannot be separated from each other when interpreting most of the lowest rovibrational states of the molecule, resulting in effective rotational constants drastically different from the equilibrium ones even for the ground vibrational state (or the ground vibrational state manifold), (d) classification of the rovibrational states requires the use of permutation-inversion symmetry and MS groups instead of point-group symmetry (applicable for semirigid molecules with a well-defined equilibrium structure), with different irreducible representations and even more unusual (for those used to electronic-structure theory) degeneracies, and (e) some (perhaps the majority) of the rovibrational eigenstates assigned to a vibrational parent state exhibit unconventional (in the most striking cases "negative") rotational contributions.

There are a number of molecular systems which clearly exhibit some (but not all) of the characteristics of quasistructural molecules. For example, in the case of pseudorotation, mutation of a vibrational dof into a rotational one takes place, while for quasilinear molecules, it is also customary to treat at least one vibrational motion together with the rotational ones. These are not quasistructural molecules.

Closed-shell molecules exhibiting quasistructural behavior include neutral species, such as dimethyl acetylene, charged species, such as H_5^+ and CH_5^+ and their deuterated analogues, vdW complexes, such as $CH_4{\cdot}H_2O$, and molecular complexes held together by HaBs, like $CF_3Cl{\cdot}CH_3F$. It is likely that as experimental techniques progress further a lot more chemical systems will be observed which exhibit quasistructural behavior. Interpretation of these measurements will depend heavily both

on highly accurate variational computations, employing Hamiltonians built upon internal coordinates, as well as sophisticated modeling efforts.

ACKNOWLEDGMENTS

This paper is dedicated to the memory of Professor Ken Hedberg, who introduced one of the authors (A.G.C.) to the wondrous world of structure determinations. The authors would like to thank NKFIH (grants no. K119658 and PD124699) for supporting part of the research described. This research was also supported by the European Union and the State of Hungary and cofinanced by the European Regional Development Fund (Grant No. VEKOP-2.3.2-16-2017-00014). The authors also thank all their coworkers for their contributions to the original publications whose results are quoted extensively in Section 6.

CONFLICT OF INTEREST

The authors have declared no conflicts of interest for this article.

RELATED WIREs ARTICLE

Fluctional molecules
Theory and simulation of atom tunneling in chemical reactions
Reactions that involve tunneling by carbon and the role that calculations have played in their study

ORCID

Attila G. Császár https://orcid.org/0000-0001-5640-191X
Csaba Fábri https://orcid.org/0000-0001-9746-1548
János Sarka https://orcid.org/0000-0003-4269-0727

REFERENCES

1. Born M, Heisenberg W. Zur Quantentheorie der Molekeln. *Ann Phys*. 1924;*379*:1–31.
2. Born M, Oppenheimer JR. Zur Quantentheorie der Molekeln. *Ann Phys*. 1927;*389*:457–484.
3. Woolley RG. Quantum theory and molecular structure. *Adv Phys*. 1976;*25*:27–52.
4. Landau LD, Lifshitz EM. *Quantum mechanics*. 3rd ed. Oxford: Pergamon, 1977.
5. Primas H. *Chemistry, quantum mechanics and reductionism: Perspectives in theoretical chemistry*. Berlin: Springer-Verlag, 1981.
6. Boggs JE. The integration of structure determination by computation, electron diffraction and microwave spectroscopy. *J Mol Struct*. 1983;*97*:1–16.
7. Sutcliffe BT, Woolley RG. Molecular structure calculations without clamping the nuclei. *Phys Chem Chem Phys*. 2005;*7*:3664–3676.
8. Sutcliffe BT. To what question is the clamped-nuclei electronic potential the answer? *Theor Chem Acc*. 2010;*127*:121–131.
9. Mátyus E, Hutter J, Müller-Herold U, Reiher M. On the emergence of molecular structure. *Phys Rev A*. 2011;*83*:052512.
10. Löwdin P-O. In: Maruani J, editor. *Molecules in physics, chemistry, and biology*. Volume II. Dordrecht: Kluwer Academic Publisher, 1988; p. 3.
11. Sutcliffe BT. Some observations on P.-O. Löwdin's definition of a molecule. *Int J Quant Chem*. 2002;*90*:66–79.
12. IUPAC Gold Book website. Available from: http://goldbook.iupac.org.
13. Demaison J, Boggs JE, Császár AG, editors. *Equilibrium molecular structures*. Boca Raton, FL: CRC Press, 2011.
14. Born M, Huang K. *Dynamical theory of crystal lattices*. New York, NY: Oxford University Press, 1954.
15. Murrell JN, Carter S, Farantos SC, Huxley P, Varandas AJC. *Molecular potential energy surfaces*. New York, NY: Wiley, 1984.
16. Mezey PG. *Potential energy hypersurfaces*. Elsevier: New York, NY, 1987.
17. Butlerov AM. Einiges über die chemische Structur der Körper. *Z Chem Pharm*. 1861;*4*:549–560.
18. Jahn HA, Teller E. Stability of polyatomic molecules in degenerate electronic states. I. Orbital degeneracy. *Proc R Soc London Ser A*. 1937;*161*:220–235.
19. von Busch H, Dev V, Eckel H-A, et al. Unambiguous proof for Berry's phase in the sodium trimer: Analysis of the transition $AE'' \leftarrow XE'$. *Phys Rev Lett*. 1998;*81*:4584–4587.
20. Bersuker IB. *The Jahn–Teller effect*. Cambridge University Press: Cambridge, 2006.
21. Wörner HJ, Qian X, Merkt F. Jahn-Teller effect in tetrahedral symmetry: Large-amplitude tunneling motion and rovibronic structure of CH_4^+ and CD_4^+. *J Chem Phys*. 2007;*126*:144305.
22. Hedberg K. Fifty years of gas-phase electron-diffraction structure research: A personal retrospective. *Struct Chem*. 2005;*16*:93–109.
23. Czakó G, Mátyus E, Császár AG. Bridging theory with experiment: A benchmark study of thermally averaged structural and effective spectroscopic parameters of the water molecule. *J Phys Chem A*. 2009;*113*:11665–11678.

24. Szabó I, Fábri C, Czakó G, Mátyus E, Császár AG. Temperature-dependent, effective structures of the $^{14}NH_3$ and $^{14}ND_3$ molecules. *J Phys Chem A*. 2012;*116*:4356–4362.
25. Mathias G, Ivanov SD, Witt A, Baer MD, Marx D. Infrared spectroscopy of fluxional molecules from (ab initio) molecular dynamics: Resolving large-amplitude motion, multiple conformations, and permutational symmetries. *J. Chem Theory Comput*. 2012;*8*:224–234.
26. Ivanov SD, Witt A, Marx D. Theoretical spectroscopy using molecular dynamics: Theory and application to CH_5^+ and its isotopologues. *Phys Chem Chem Phys*. 2013;*15*:10270.
27. Vager Z, Naaman R, Kanter EP. Coulomb explosion imaging of small molecules. *Science*. 1989;*244*:426–431.
28. Yamanouchi K. LASER chemistry and physics: The next frontier. *Science*. 2002;*295*:1659–1660.
29. Légaré F, Lee KF, Litvinyuk IV, et al. Laser Coulomb-explosion imaging of small molecules. *Phys Rev A*. 2005;*71*:013415.
30. Kroto HW. *Molecular rotation spectra*. New York, NY: Dover, 1992.
31. Wilson EB Jr, Decius JC, Cross PC. *Molecular vibrations*. New York, NY: McGraw-Hill, 1955.
32. Nielsen HH. The vibration-rotation energies of molecules. *Rev Mod Phys*. 1951;*23*:90–136.
33. Mills IM. Vibration-rotation structure in asymmetric and symmetric-top molecules. *Molecular spectroscopy: Modern research*. New York, London: Academic Press. 1972;p. 115–140.
34. Clabo DA Jr, Allen WD, Remington RB, Yamaguchi Y, Schaefer HF III. A systematic study of molecular vibrational anharmonicity and vibration–rotation interaction by self-consistent-field higher-derivative methods. Asymmetric top molecules. *Chem Phys*. 1988;*123*:187–239.
35. Allen WD, Yamaguchi Y, Császár AG, Clabo DA Jr, Remington RB, Schaefer HF III. A systematic study of molecular vibrational anharmonicity and vibration-rotation interaction by self-consistent-field higher-derivative methods. Linear polyatomic molecules. *Chem Phys*. 1990;*145*:427–466.
36. Morse PM. Diatomic molecules according to the wave mechanics. II. Vibrational levels. *Phys Rev*. 1929;*34*:57–64.
37. Mátyus E, Fábri C, Szidarovszky T, Czakó G, Allen WD, Császár AG. Assigning quantum labels to variationally computed rotational-vibrational eigenstates of polyatomic molecules. *J Chem Phys*. 2010;*133*:034113.
38. Herzberg G. *Molecular spectra and molecular structure*. Vol 1–3. Melbourne: Van Nostrand Reinhold, 1945.
39. Townes CH, Schawlow AL. *Microwave spectroscopy*. New York, NY: McGraw Hill, 1955.
40. Gordy W, Cook RL. *Microwave molecular spectra*. 3rd ed. New York, NY: Wiley, 1984.
41. Bunker PR, Jensen P. *Molecular symmetry and spectroscopy*. Ottawa: NRC Research Press, 1998.
42. Merkt F, Quack M. In: Quack M, Merkt F, editors. *Handbook of high-resolution spectroscopy*. Chichester: Wiley, 2011.
43. Pokutnyi SI. Theory of excitons and excitonic quasimolecules formed from spatially separated electrons and holes in quasi - zero - dimensional nanosystems. *Optics*. 2014;*3*:10–21.
44. Pokutnyi SI, Kulchin YN, Dzyuba VP, Amosov AV. Biexciton in nanoheterostructures of dielectric quantum dots. *J Nanophoton*. 2016;*10*:036008.
45. Cope AC, Hardy EM. The introduction of substituted vinyl groups. V. A rearrangement involving the migration of an allyl group in a three-carbon system 1. *J Am Chem Soc*. 1940;*62*:441–444.
46. Doering W, Roth W. A rapidly reversible degenerate cope rearrangement. *Tetrahedron*. 1963;*19*:715–737.
47. Kilpatrick JE, Pitzer KS, Spitzer R. The thermodynamics and molecular structure of cyclopentane 1. *J Am Chem Soc*. 1947;*69*:2483–2488.
48. Longuet-Higgins HC. The symmetry groups of non-rigid molecules. *Mol Phys*. 1963;*6*:445–460.
49. Hougen JT. Strategies for advanced applications of permutation–inversion groups to the microwave spectra of molecules with large amplitude motions. *J Mol Spectrosc*. 2009;*256*:170–185.
50. Demaison J, Császár AG, Kleiner I, Mollendal H. Equilibrium vs ground-state planarity of the CONH linkage. *J Phys Chem A*. 2007;*111*:2574–2586.
51. Fábri C, Sarka J, Császár AG. Communication: Rigidity of the molecular ion H_5^+. *J Chem Phys*. 2014;*140*:051101.
52. Sarka J, Fábri C, Szidarovszky T, Császár AG, Lin Z, McCoy AB. Modelling rotations, vibrations, and rovibrational couplings in astructural molecules—A case study based on the H_5^+ molecular ion. *Mol Phys*. 2015;*113*:1873–1883.
53. Sarka J, Császár AG. Interpretation of the vibrational energy level structure of the astructural molecular ion H_5^+ and all of its deuterated isotopomers. *J Chem Phys*. 2016;*144*:154309.
54. Sarka J, Császár AG, Althorpe SC, Wales DJ, Mátyus E. Rovibrational transitions of the methane–water dimer from intermolecular quantum dynamical computations. *Phys Chem Chem Phys*. 2016;*18*:22816–22826.
55. Fábri C, Quack M, Császár AG. On the use of nonrigid-molecular symmetry in nuclear motion computations employing a discrete variable representation: A case study of the bending energy levels of CH_5^+. *J Chem Phys*. 2017;*147*:134101.
56. Fábri C, Császár AG. Vibrational quantum graphs and their application to the quantum dynamics of CH5+. *Phys Chem Chem Phys*. 2018;*20*:16913–16917.
57. Császár AG, Fábri C, Szidarovszky T, Mátyus E, Furtenbacher T, Czakó G. Fourth age of quantum chemistry: Molecules in motion. *Phys Chem Chem Phys*. 2012;*13*:1085–1106.
58. Mátyus E, Szidarovszky T, Császár AG. Modelling non-adiabatic effects in H_3^+: Solution of the rovibrational Schrödinger equation with motion-dependent masses and mass surfaces. *J Chem Phys*. 2014;*114*:154111.
59. Šmydke J, Császár AG. On the use of reduced-density matrices for the semi-automatic assignment of vibrational states. *Mol Phys*. 2019;*117*:1682–1693.
60. Lewis GN. *Valence and the structure of molecules*. New York, NY: Chemical Catalog Co., 1923.
61. Adams J. The fourth age of research. *Nature*. 2013;*497*:557–560.

62. Polyansky OL, Császár AG, Shirin SV, et al. High-accuracy ab initio rotation-vibration transitions for water. *Science*. 2003;*299*:539–542.
63. Hall JL. Nobel lecture: Defining and measuring optical frequencies. *Rev Mod Phys*. 2006;*78*:1279–1295.
64. Hänsch TW. Nobel lecture: Passion for precision. *Rev Mod Phys*. 2006;*78*:1297–1309.
65. Cozijn F, Dupré P, Salumbides E, Eikema K, Ubachs W. Sub-Doppler frequency metrology in HD for tests of fundamental physics. *Phys Rev Lett*. 2018;*120*:153002.
66. Gordon I, Rothman L, Hill C, et al. The HITRAN2016 molecular spectroscopic database. *J Quant Spectrosc Radiat Transfer*. 2017;*203*:3–69.
67. Rydberg R. Graphic representation of results of band spectroscopy. *Zs Phys*. 1931;*73*:376–385.
68. Klein O. Calculation of potential curves for diatomic molecules with help of spectral terms. *Zs Phys*. 1932;*76*:226–235.
69. Rees ALG. The calculation of potential-energy curves from band-spectroscopic data. *Proc. Phys Soc (London)*. 1947;*59*:998–1008.
70. Szidarovszky T, Császár AG. Grid-based empirical improvement of molecular potential energy surfaces. *J Phys Chem A*. 2014;*118*: 6256–6265.
71. Helgaker T, Jorgensen P, Olsen J. *Molecular electronic-structure theory*. Chichester: Wiley, 2000.
72. Bell RP. *The tunnel effect in chemistry*. New York, NY: Chapman and Hall, 1980.
73. Schreiner PR, Reisenauer HP, Pickard FC, et al. Capture of hydroxymethylene and its fast disappearance through tunnelling. *Nature*. 2008; *453*:906–909.
74. Kästner J. Theory and simulation of atom tunneling in chemical reactions. *WIREs Comput Mol Sci*. 2014;*4*:158–168.
75. Borden WT. Reactions that involve tunneling by carbon and the role that calculations have played in their study. *WIREs Comput Mol Sci*. 2016;*6*:20–46.
76. Szalay V, Császár AG, Senent ML. Symmetry analysis of internal rotation. *J Chem Phys*. 2002;*117*:6489–6492.
77. Allen WD, Bodi A, Szalay V, Császár AG. Adiabatic approximations to internal rotation. *J Chem Phys*. 2006;*124*:224310.
78. Lees R, Baker J. Torsion-vibration-rotation interactions in methanol. I. Millimeter wave spectrum. *J Chem Phys*. 1968;*48*:5299–5318.
79. Herbst E, Messer J, De Lucia FC, Helminger P. A new analysis and additional measurements of the millimeter and submillimeter spectrum of methanol. *J Mol Spectrosc*. 1984;*108*:42–57.
80. Hougen JT, Kleiner I, Godefroid M. Selection rules and intensity calculations for a C_s asymmetric top molecule containing a methyl group internal rotor. *J Mol Spectrosc*. 1994;*163*:559–586.
81. Szalay V, Császár AG, Santos J, Ortigoso J. Rho-axis-system Hamiltonian for molecules with one large amplitude internal motion. *J Chem Phys*. 2003;*118*:6801–6805.
82. Kriner WA, Rudolph HD, Tan BT. Microwave spectra of several molecular isotopes of toluene. *J Mol Spectrosc*. 1973;*48*:86–99.
83. Borst DR, Pratt DW. Toluene: Structure, dynamics, and barrier to methly group rotation in its electronically excited state. A route to IVR. *J Chem Phys*. 2000;*113*:3658–3669.
84. Lin CC, Swalen JD. Internal rotation and microwave spectroscopy. *Rev Mod Phys*. 1959;*31*:841–892.
85. Szalay V, Ortigoso J. The internal axis system of molecules with one large amplitude internal motion. *J Chem Phys*. 1998;*109*:3911–3918.
86. Xu L-H, Lees RM, Hougen JT. On the physical interpretation of torsion-rotation parameters in methanol and acetaldehyde: Comparison of global fit and *ab initio* results. *J Chem Phys*. 1999;*110*:3835–3841.
87. McKee ML. Fluctional molecules. *WIREs Comput Mol Sci*. 2011;*1*:943–951.
88. Ault A. The bullvalene story. The conception of bullvalene, a molecule that has no permanent structure. *J Chem Ed*. 2001;*78*:924–927.
89. Bauer SH, Wilcox CF. On malonaldehyde and acetylacetone: Are theory and experiment compatible? *Chem Phys Lett*. 1997;*279*:122–128.
90. Cotton FA. A half-century of nonclassical organometallic chemistry: A personal perspective. *Inorg Chem*. 2002;*41*:643–658.
91. Montgomery CD. Mechanisms of pentacoordinate pseudorotation. A molecular modeling study of PF_5. *J Chem Educ*. 2001;*78*:844–846.
92. McKee ML. In: Schleyer PVR et al., editors. *Fluxional processes in boranes and carboranes, in The encyclopedia of computational chemistry*. Chichester: Wiley, 1998.
93. Vargas A, Santarossa G, Iannuzzi M, Baiker A. Fluxionality of gold nanoparticles investigated by Born-Oppenheimer molecular dynamics. *Phys Rev B*. 2009;*80*:195421.
94. DeRosa MC, White CA, Evans CEB, Crutchley RJ. Infrared study of the class II/class III boundary in mixed-valence dinuclear ruthenium complexes. *J Am Chem Soc*. 2001;*123*:1396–1402.
95. Nesbitt DJ, Naaman R. On the apparent spectroscopic rigidity of floppy molecular systems. *J. Chem Phys*. 1989;*91*:3801–3809.
96. Bohm A, Boya LJ, Kendrick B. Derivation of the geometrical phase. *Phys Rev A*. 1991;*43*:1206–1210.
97. Bohm A, Kendrick B, Loewe ME. The berry phase in molecular physics. *Int J Quant Chem*. 1992;*41*:53–75.
98. Eckel H-A, Gress J-M, Biele J, Demtröder W. Sub-Doppler optical double-resonance spectroscopy and rotational analysis of Na_3. *J Chem Phys*. 1993;*98*:135–139.
99. Albert S, Chen Z, Fábri C, Lerch P, Prentner R, Quack M. A combined gigahertz and terahertz (FTIR) spectroscopic investigation of meta-D-phenol: Observation of tunnelling switching. *Mol Phys*. 2016;*114*:2751–2768.
100. Šmydke J, Fábri C, Sarka J, Császár AG. Rovibrational quantum dynamics of the vinyl radical and its deuterated isotopologues. *Phys Chem Chem Phys*. 2019;*21*:3453–3472.
101. Nesbitt D. Toward state-to-state dynamics in ultracold collisions: Lessons from high-resolution spectroscopy of weakly bound molecular complexes. *J Chem Rev*. 2012;*112*:5062–5072.
102. Metz MP, Szalewicz K, Sarka J, Tóbiás R, Császár AG, Mátyus E. Molecular dimers of methane clathrates: ab initio potential energy surfaces and variational vibrational states. *Phys Chem Chem Phys*. 2019;21:13504–13525.
103. Herschbach DR. Calculation of energy levels for internal torsion and over-all rotation. *J Chem Phys*. 1959;*31*:91–108.

104. Sarka J, Császár AG, Mátyus E. Rovibrational quantum dynamical computations for deuterated isotopologues of the methane–water dimer. *Phys Chem Chem Phys*. 2017;*19*:15335–15345.
105. Douslin DR, Huffman HM. The heat capacities, heats of transition, heats of fusion and entropies of cyclopentane, methylcyclopentane and methylcyclohexane. *J Am Chem Soc*. 1946;*68*:173–176.
106. Spitzer R, Pitzer KS. The heat capacity of gaseous cyclopentane, cyclohexane and methylcyclohexane. *J Am Chem Soc*. 1946;*68*:2537–2538.
107. Sax AF. On pseudorotation. *Chem Phys*. 2008;*349*:9–31.
108. Harris DO, Engerholm GG, Tolman CA, et al. Ring puckering in five-membered rings. *J Chem Phys*. 1969;*50*:2438–2445.
109. Kowalewski P, Frey H-M, Infanger D, Leutwyler S. Probing the structure, pseudorotation, and radial vibrations of cyclopentane by femtosecond rotational Raman coherence spectroscopy. *J Phys Chem A*. 2015;*119*:11215–11225.
110. Tanner K, Weber A. The pure rotational Raman spectrum of cyclopentane-d_0 and cyclopentane-d_{10}. *J Mol Spectrosc*. 1963;*10*:381–398.
111. Manz J. Rotating molecules trapped in pseudorotating cages. *J Am Chem Soc*. 1801–1806;*1980*:102.
112. Devonshire AF. The rotation of molecules in fields of octahedral symmetry. *Proc R Soc London, Ser A*. 1936;*153*:601–621.
113. Benoit DM, Lauvergnat D, Scribano Y. Does cage quantum delocalisation influence the translation-rotational bound states of molecular hydrogen in clathrate hydrate? *Mol Phys*. 2018;*212*:533–546.
114. Bloodworth S, Sitinova G, Alom S, et al. First synthesis and characterization of CH_4 C_{60}. *Angew Chem Int Ed*. 2019;*58*:5038–5043.
115. Signorell R, Merkt F. The first rotationally resolved spectrum of CH_4^+. *J Chem Phys*. 1999;*110*:2309–2311.
116. Signorell R, Sommavilla M, Merkt F. Jahn–Teller distortion in $CD_2H_2^+$ from a rotationally resolved photoelectron spectrum. *Chem Phys Lett*. 1999;*312*:139–148.
117. Wörner HJ, van der Veen R, Merkt F. Jahn-Teller effect in the methane cation: Rovibronic structure and the geometric phase. *Phys Rev Lett*. 2006;*97*:173003.
118. Bunker PR, Landsberg BM. The rigid bender and semirigid bender models for the rotation-vibration Hamiltonian. *J Mol Spectrosc*. 1977;*67*:374–385.
119. Bunker PR, Landsberg BM, Winnewisser BP. HCNO as a semirigid bender. *J Mol Spectrosc*. 1979;*74*:9–25.
120. McKellar ARW, Bunker PR, Sears TJ, Evenson KM, Saykally RJ, Langhoff SR. Far infrared laser magnetic resonance of singlet methylene: Singlet-triplet perturbations, singlet-triplet transitions, and the singlet-triplet splitting. *J Chem Phys*. 1983;*79*:5251–5264.
121. Furtenbacher T, Czakó G, Sutcliffe BT, Császár AG, Szalay V. The methylene saga continues: Stretching fundamentals and zero-point energy of $\tilde{X}^3B_1$ CH_2. *J Mol Struct*. 2006;*780-781*:283–294.
122. Jensen P, Bunker PR. The potential surface and stretching frequencies of $\tilde{X}^3B_1$ methylene (CH_2) determined from experiment using the Morse oscillator-rigid bender internal dynamics Hamiltonian. *J Chem Phys*. 1988;*89*:1327–1332.
123. Schaefer HF III. Methylene: A paradigm for computational quantum chemistry. *Science*. 1986;*231*:1100–1107.
124. Herzberg G. The spectra and structures of free methyl and free methylene. *Proc R Soc Lond A*. 1961;*262*:291–317.
125. Sherrill CD, Leininger ML, van Huis TJ, Schaefer HF III. Structures and vibrational frequencies in the full configuration interaction limit: Predictions for four electronic states of methylene using a triple-zeta plus double polarization (TZ2P) basis. *J Chem Phys*. 1998;*108*:1040–1049.
126. Császár AG, Leininger ML, Szalay V. The enthalpy of formation of CH_2. *J Chem Phys*. 2003;*118*:10631–10642.
127. Ruscic B, Boggs JE, Burcat A, et al. IUPAC critical evaluation of thermochemical properties of selected radicals. Part I. *J Phys Chem Ref Data*. 2005;*34*:573–656.
128. Fusina L, Mills IM. Carbon suboxide: The vibrational dependence of the ν_7 bending potential function. *J Mol Spectrosc*. 1980;*79*:123–131.
129. Bunker PR. Carbon suboxide as a semirigid bender. *J Mol Spectrosc*. 1980;*80*:422–437.
130. Caminati W, Maris A, Dell'Erba A, Favero PG. Dynamical behavior and dipole-dipole interactions of tetrafluoromethane-water. *Angew. Chem., Int. Ed.* 2006, *45*, 6711–6714.
131. Evangelisti L, Feng G, Ecija P, Cocinero E, Castano F, Caminati W. Dynamical behavior and dipole-dipole interactions of tetrafluoromethane-water. *Angew Chem, Int Ed*. 2011;*50*:7807–7810.
132. Feng G, Evangelisti L, Gasparini N, Caminati W. On the Cl···N halogen bond: A rotational study of CF_3Cl···NH_3. *Chem A Eur J*. 2012;*18*:1364–1368.
133. Maris A, Favero PG, Velino B, Caminati W. Pyridine–CF_4: A molecule with a rotating cap. *J Phys Chem A*. 2013;*117*:11289–11292.
134. Gou Q, Spada L, Cocinero EJ, Caminati W. Halogen-halogen links and internal dynamics in adducts of freons. *J Phys Chem Lett*. 2014;*5*:1591–1595.
135. Evangelisti L, Feng G, Gou Q, Grabow J-U, Caminati W. Halogen bond and free internal rotation: The microwave spectrum of CF3Cl–dimethyl ether. *J Phys Chem A*. 2014;*118*:579–582.
136. Bauder A, Mathier E, Meyer R, Ribeaud M, Günthard HH. Theory of rotation and torsion spectra for a semi-rigid model of molecules with an internal rotor of C_{2v} symmetry. *Mol Phys*. 1968;*15*:597–614.
137. Ribeaud M, Bauder A, Günthard HH. Structure relaxation during internal rotation of the nitro group in nitrobenzene. *Mol Phys*. 1972;*23*:235–248.
138. Doering W, Wang Y. Perturbation of Cope's rearrangement: 1,3,5-Triphenylhexa-1,5-diene. Chameleonic or centauric transition region? *J Am Chem Soc*. 1999;*121*:10112–10118.
139. Navarro-Vázquez A, Prall M, Schreiner PR. Cope reaction families: To be or not to be a biradical. *Org Lett*. 2004;*6*:2981–2984.
140. Claisen L. Über Umlagerung von Phenol-allyl-äthern in *C*-Allyl-phenole. *Chem Ber*. 1912;*42*:3157–3166.
141. Rhoads SJ, Raulius R. The Claisen and Cope rearrangements. *Org React*. 1975;*22*:1.
142. Bergman RG. Reactive 1,4-dehydroaromatics. *Acc Chem Res*. 1973;*6*:25–31.

143. Myers AG, Kuo EY, Finney NS. Thermal generation of α,3-dehydrotoluene from (Z)-1,2,4-heptatrien-6-yne. *Am Chem Soc*. 1989;*111*: 8057–8059.
144. Zhang X, Hrovat DA, Borden WT. Calculations predict that carbon tunneling allows the degenerate Cope rearrangement of semibullvalene to occur rapidly at cryogenic temperatures. *Org Lett*. 2010;*12*:2798–2801.
145. Schleif T, Mieres-Perez J, Henkel S, Ertelt M, Borden WT, Sander W. The Cope rearrangement of 1,5-dimethylsemibullvalene-2(4)-d_1: Experimental evidence for heavy-atom tunneling. *Angew Chem Int Ed*. 2017;*56*:10746–10749.
146. Whitman DW, Carpenter BK. Limits on the activation parameters for automerization of cyclobutadiene-1,2-d_2. *J Am Chem Soc*. 1983;*105*: 1700–1701.
147. Carpenter BK. Heavy-atom tunneling as the dominant pathway in a solution-phase reaction? Bond shift in antiaromatic annulenes. *J Am Chem Soc*. 1700–1701;*1983*:105.
148. Sander W, Bucher G, Reichel F, Cremer D. 1H-Bicyclo[3.1.0]hexa-3,5-dien-2-one. A strained 1,3-bridged cyclopropene. *J Am ChemSoc*. 1991;*113*:5311–5322.
149. Zuev PS, Sheridan RS, Albu TV, Truhlar DG, Hrovat DA, Borden WT. Carbon tunneling from a single quantum state. *Science*. 2003;*299*: 867–870.
150. Inui H, Sawada K, Oishi S, Ushida K, McMahon RJ. Aryl nitrene rearrangements: Spectroscopic observation of a benzazirine and its ring expansion to a ketenimine by heavy-atom tunneling. *J Am Chem Soc*. 2013;*135*:10246–10249.
151. Huang M-J, Wolfsberg M. Tunneling in the automerization of cyclobutadiene. *J Am Chem Soc*. 1984;*106*:4039–4040.
152. Cheng TC, Bandyipadyay B, Wang Y, et al. Shared-proton mode lights up the infrared spectrum of fluxional cations H_5^+ and D_5^+. *J Phys Chem Lett*. 2010;*1*:758–762.
153. Cheng TC, Jiang L, Asmis KR, et al. Mid- and far-IR spectra of H_5^+ and D_5^+ compared to the predictions of anharmonic theory. *J Phys Chem Lett*. 2012;*3*:3160–3166.
154. Acioli PH, Xie Z, Braams BJ, Bowman JM. Vibrational ground state properties of H_5^+ and its isotopomers from diffusion Monte Carlo calculations. *J Chem Phys*. 2008;*128*:104318.
155. de Tudela RP, Barragán P, Prosmiti R, Villarreal P, Delgado-Barrio G. Internal proton transfer and H_2 rotations in the H_5^+ cluster: a marked influence on its thermal equilibrium state. *J Phys Chem A*. 2011;*115*:2483–2488.
156. Barragán P, de Tudela RP, Prosmiti R, Villarreal P, Delgado-Barrio G. Path integral Monte Carlo studies of the H_5^+/D_5^+ clusters using ab initio potential surfaces. *Phys Scr*. 2011;*84*:028109.
157. McGuire BA, Wang Y, Bowman JM, Widicus Weaver SL. Do H_5^+ and its isotopologues have rotational spectra? *J Phys Chem Lett*. 2011;*2*: 1405–1407.
158. Aguado A, Sanz-Sanz C, Villareal P, Roncero O. Simulation of the infrared predissociation spectra of H_5^+. *Phys Rev A*. 2012;*85*:032514.
159. Valdes A, Prosmiti R, Delgado-Barrio G. Quantum-dynamics study of the H_5^+ cluster: Full dimensional benchmark results on its vibrational states. *J Chem Phys*. 2012;*136*:104302.
160. Valdes A, Prosmiti R, Delgado-Barrio G. Vibrational dynamics of the H_5^+ and its isotopologues from multiconfiguration time-dependent Hartree calculations. *J Chem Phys*. 2012;*137*:214308.
161. Lin Z, McCoy AB. Signatures of large-amplitude vibrations in the spectra of H_5^+ and D_5^+. *J Phys Chem Lett*. 2012;*3*:3690–3696.
162. Lin Z, McCoy AB. Investigation of the structure and spectroscopy of H_5^+ using diffusion Monte Carlo. *J Phys Chem A*. 2013;*117*: 11725–11736.
163. Song H, Lee S-Y, Yang M, Lu Y. Full-dimensional quantum calculations of the vibrational states of H_5^+. *J Chem Phys*. 2013;*138*:124309.
164. Valdés A, Prosmiti R. Theoretical investigation of the infrared spectra of the H_5^+ and D_5^+ cations. *J Phys Chem A*. 2013;*117*:9518–9524.
165. Valdés A, Prosmiti R. Theoretical predictions on the role of the internal H_3^+ rotation in the IR spectra of the H_5^+ and D_5^+ cations. *Phys Chem Chem Phys*. 2014;*16*:6217–6224.
166. Lin Z, McCoy AB. The role of large-amplitude motions in the spectroscopy and dynamics of H_5^+. *J Chem Phys*. 2014;*140*:114305.
167. Marlett ML, Lin Z, McCoy AB. Rotation/torsion coupling in H_5^+, D_5^+, H_4D^+, and HD_4^+ using diffusion Monte Carlo. *J Phys Chem A*. 2015; *119*:9405–9413.
168. Lin Z, McCoy AB. Probing the relationship between large-amplitude motions in H_5^+ and proton exchange between H_3^+ and H_2. *J Phys Chem A*. 2015;*119*:12109–12118.
169. Olah GA. My search for carbocations and their role in chemistry. *Les Prix Nobel en*. Vol 1994, 1994;p. 149–176.
170. Marx D, Parrinello M. Structural quantum effects and three-centre two-electron bonding in CH_5^+. *Nature*. 1995;*375*:216–218.
171. White ET, Tang J, Oka T. CH_5^+: The infrared spectrum observed. *Science*. 1999;*284*:135–137.
172. Asvany O, Padma Kumar P, Redlich B, Hegemann I, Schlemmer S, Marx D. Understanding the infrared spectrum of bare CH_5^+. *Science*. 2005;*309*:1219–1222.
173. Ivanov SD, Asvany O, Witt A, et al. Quantum-induced symmetry breaking explains infrared spectra of CH_5^+ isotopologues. *Nature Chem*. 2010;*2*:298–302.
174. Asvany O, Yamada KMT, Brünken S, Potapov A, Schlemmer S. Experimental ground-state combination differences of CH_5^+. *Science*. 2015; *347*:1346–1349.
175. Brackertz S, Schlemmer S, Asvany O. Searching for new symmetry species of CH_5^+—From lines to states without a model. *J Mol Spectrosc*. 2017;*342*:73–82.

176. Müller H, Kutzelnigg W, Noga J, Klopper W. CH_5^+: The story goes on. An explicitly correlated coupled-cluster study. *J Chem Phys*. 1997;*106*:1863–1869.
177. Schreiner PR, Kim S-J, Schaefer HF III, von Ragué Schleyer P. CH_5^+: The never-ending story or the final word? *J Chem Phys*. 1993;*99*:3716–3720.
178. Kolbuszewski M, Bunker PR. Potential barriers, tunneling splittings, and the predicted $J = 1 \leftarrow 0$ spectrum of CH_5^+. *J Chem Phys*. 1996;*105*:3649–3653.
179. Dalton B. Classification of the states of non-rigid molecules. *J Mol Phys*. 1966;*11*:265–285.
180. Dalton BJ. Nonrigid molecule effects on the rovibronic energy levels and spectra of phosphorous pentafluoride. *J Chem Phys*. 1971;*54*:4745–4762.
181. Wigner EP. *Group theory and its application to the quantum mechanics of atomic spectra*. Academic Press: New York, NY, 1959.
182. Brown A, McCoy AB, Braams BJ, Jin Z, Bowman JM. Quantum and classical studies of vibrational motion of CH_5^+ on a global potential energy surface obtained from a novel ab initio direct dynamics approach. *J Chem Phys*. 2004;*121*:4105–4116.
183. Jin Z, Braams BJ, Bowman JM. An ab initio based global potential energy surface describing $CH_5^+ \rightarrow CH_3^+ + H_2$. *J Phys Chem A*. 2006;*110*:1569–1574.
184. Bunker P. A preliminary study of the proton rearrangement energy levels and spectrum of CH_5^+. *J Mol Spectrosc*. 1996;*176*:297–304.
185. East ALL, Bunker PR. A general rotation-contortion Hamiltonian with structure relaxation: Application to the precessing internal rotor model. *J Mol Spectrosc*. 1997;*183*:157–162.
186. East ALL, Kolbuszewski M, Bunker PR. Ab initio calculation of the rotational spectrum of CH_5^+ and CD_5^+. *J Phys Chem A*. 1997;*101*:6746–6752.
187. Bunker P, Ostojić B, Yurchenko S. A theoretical study of the millimeterwave spectrum of CH_5^+. *J Mol Struct*. 2004;*695-696*:253–261.
188. Huang X, McCoy AB, Bowman JM, et al. Quantum deconstruction of the infrared spectrum of CH_5^+. *Science*. 2006;*311*:60–63.
189. Deskevich MP, McCoy AB, Hutson JM, Nesbitt DJ. Large-amplitude quantum mechanics in polyatomic hydrides. II. A particle-on-a-sphere model for XH_n ($n = 4, 5$). *J Chem Phys*. 2008;*128*:094306.
190. Johnson LM, McCoy AB. Evolution of structure in CH_5^+ and its deuterated analogues. *J Phys Chem A*. 2006;*110*:8213–8220.
191. Hinkle CE, McCoy AB. Characterizing excited states of CH_5^+ with diffusion Monte Carlo. *J Phys Chem A*. 2008;*112*:2058–2064.
192. Hinkle CE, McCoy AB. Theoretical investigations of mode mixing in vibrationally excited states of CH_5^+. *J Phys Chem A*. 2009;*113*:4587–4597.
193. Hinkle CE, McCoy AB. Minimum energy path diffusion Monte Carlo approach for investigating anharmonic quantum effects: Applications to the $CH_3^+ + H_2$ reaction. *J Phys Chem Lett*. 2010;*1*:562–567.
194. Hinkle CE, McCoy AB. Isotopic effects on the dynamics of the $CH_3^+ + H_2 \rightarrow CH_5^+ \rightarrow CH_3^+ + H_2$ reaction. *J Phys Chem A*. 2012;*116*:4687–4694.
195. Petit AS, Ford JE, McCoy AB. Simultaneous evaluation of multiple rotationally excited states of H_3^+, H_3O^+, and CH_5^+ using diffusion Monte Carlo. *J Phys Chem A*. 2014;*118*:7206–7220.
196. Wang X-G, Carrington T Jr. Vibrational energy levels of CH_5^+. *J Chem Phys*. 2008;*129*:234102.
197. Wodraszka R, Manthe U. CH_5^+: Symmetry and the entangled rovibrational quantum states of a fluxional molecule. *J Phys Chem Lett*. 2015;*6*:4229–4232.
198. Wang X-G, Carrington T. Calculated rotation-bending energy levels of CH_5^+ and a comparison with experiment. *J Chem Phys*. 2016;*144*:204304.
199. Schmiedt H, Schlemmer S, Jensen P. Symmetry of extremely floppy molecules: Molecular states beyond rotation-vibration separation. *J Chem Phys*. 2015;*143*:154302.
200. Kuchment P. Graph models for waves in thin structures. *Wave Random Media*. 2002;*12*:R1–R24.
201. Berkolaiko G, Kuchment P. Introduction to Quantum Graphs. *Mathematical Surveys and Monographs*. Vol 186. Providence, RI: American Mathematical Society, 2013.
202. Pauling L. The diamagnetic anisotropy of aromatic molecules. *J Chem Phys*. 1936;*4*:673–677.
203. Kuhn H. Quantenmechanische Behandlung von Farbstoffen mit Verzweigtem Elektronengas. *Helv Chim Acta*. 1949;*32*:2247–2272.
204. Ruedenberg K, Scherr CW. Free-electron network model for conjugated systems. I. Theory. *J Chem Phys*. 1953;*21*:1565–1581.
205. Scherr CW. Free-electron network model for conjugated systems. II. Numerical calculations. *J Chem Phys*. 1953;*21*:1582–1596.
206. Richardson MJ, Balazs NL. On the network model of molecules and solids. *Ann Phys*. 1972;*73*:308–325.
207. Kottos T, Smilansky U. Quantum chaos on graphs. *Phys Rev Lett*. 1997;*79*:4794–4797.
208. Kottos T, Smilansky U. Chaotic scattering on graphs. *Phys Rev Lett*. 2000;*85*:968–971.
209. Gnutzmann S, Smilansky U. Quantum graphs: Applications to quantum chaos and universal spectral statistics. *Adv Phys*. 2006;*55*:527–625.
210. Schanz H, Smilansky U. Periodic-orbit theory of Anderson localization on graphs. *Phys Rev Lett*. 2000;*84*:1427–1430.
211. Montambaux G. Mesoscopic physics on graphs. *Phys Usp*. 2001;*44*:65–68.
212. Schmiedt H, Jensen P, Schlemmer S. Collective molecular superrotation: A model for extremely flexible molecules applied to protonated methane. *Phys Rev Lett*. 2016;*117*:223002.
213. Schmiedt H, Jensen P, Schlemmer S. Rotation-vibration motion of extremely flexible molecules – The molecular superrotor. *Chem Phys Lett*. 2017;*672*:34–46.
214. Schmiedt H, Jensen P, Schlemmer S. The role of angular momentum in the superrotor theory for rovibrational motion of extremely flexible molecules. *J Mol Spectrosc*. 2017;*342*:132–137.

215. Zurawski B, Ahlrichs R, Kutzelnigg W. Have the ions $C_2H_3^+$ and $C_2H_5^+$ classical or non-classical structure? *Chem Phys Lett*. 1973;*21*:309–313.
216. Kanter EP, Vager Z, Both G, Zajfman D. A measurement of the low energy stereostructure of protonated acetylene, $C_2H_3^+$. *J Chem Phys*. 1986;*85*:7487–7488.
217. Vager Z, Zajfman D, Graber T, Kanter EP. Experimental evidence for anomalous nuclear delocalization in $C_2H_3^+$. *Phys Rev Lett*. 1993;*71*:4319.
218. Knoll L, Vager Z, Marx D. Experimental versus simulated Coulomb-explosion images of flexible molecules: Structure of protonated acetylene $C_2H_3^+$. *Phys Rev A*. 2003;*67*:022506.
219. Car R, Parrinello M. Unified approach for molecular dynamics and density-functional theory. *Phys Rev Lett*. 1985;*55*:2471.
220. Marx D, Tuckerman ME, Martyna GJ. Quantum dynamics via adiabatic ab initio centroid molecular dynamics. *Comput Phys Commun*. 1999;*118*:166–184.
221. Duncan MA. Infrared laser spectroscopy of mass-selected carbocations. *J Phys Chem A*. 2012;*116*:11477–11491.
222. Dore L, Cohen RC, Schmuttenmaer CA, et al. Far infrared vibration-rotation-tunneling spectroscopy and internal dynamics of methane-water: A prototypical hydrophobic system. *J Chem Phys*. 1994;*100*:863–876.
223. di Lauro C, Bunker PR, Johns JWC, McKellar ARW. The rotation-torsion structure in the ν_{11}/ν_{15} (G_s) methyl rocking fundamental band of dimethylacetylene. *J Mol Spectrosc*. 1997;*184*:177–185.
224. Crawford BL. Infra-red and Raman spectra of polyatomic molecules IX. Dimethyl acetylene, C_4H_6. *J Chem Phys*. 1939;*7*:555–562.
225. Yost DM, Osborne DW, Garner CS. The heat capacity, entropy, and heats of transition, fusion, and vaporization of dimethylacetylene. Free rotation in the dimethylacetylene molecule. *J Am Chem Soc*. 1941;*63*:3492–3496.
226. Mills IM, Thompson HW. Internal rotation in dimethyl acetylene. *Proc R Soc London, Ser A*. 1954;*226*:306–314.
227. Bunker PR, Longuet-Higgins HC. The infra-red spectrum of dimethylacetylene and the torsional barrier. *Proc R Soc London, Ser A*. 1964;*280*:340–352.
228. Bauder A. In: Quack M, Merkt F, editors. *Handbook of High-resolution Spectroscopy*. Chichester: Wiley, 2011; p. 57–116.

How to cite this article: Császár AG, Fábri C, Sarka J. Quasistructural molecules. *WIREs Comput Mol Sci*. 2020;10:e1432. https://doi.org/10.1002/wcms.1432

APPENDIX A. A Model Hamiltonian Coupling Vibration to Rotations

We start with the four-dimensional model Hamiltonian

$$\hat{H} = -a\hat{p}^2 + B\hat{J}^2 + (A-B)\hat{J}_z^2 + \alpha\hat{p}\hat{J}_z + \hat{V} \tag{A1}$$

describing a symmetric-top molecule with a torsional dof coupled to one of the rotational dofs. In Equation (A1), $\hat{p} = -\mathrm{i}\frac{\partial}{\partial\varphi}$ (φ is the torsional angle), a depends on the moment of inertia of the internal rotor, the three components of the overall body-fixed angular momentum $\hat{J}$ are denoted by $\hat{J}_i$, A and B are the rotational constants, and α is the rovibrational coupling strength. $\hat{V}$ is the potential energy depending solely on φ and has typically multiple minima. Three cases must be distinguished: (a) no barrier ($\hat{V} = 0$), (b) low barrier, and (c) high barrier. Note that considerations similar to those described in this appendix are presented in References 40 and 228.

If the internal rotation is free ($\hat{V} = 0$), the eigenfunctions of $\hat{H}$ take the form

$$|kJK\rangle = |k\rangle\,|JK\rangle \tag{A2}$$

where $|k\rangle$ corresponds to $\frac{1}{\sqrt{2\pi}}\exp(\mathrm{i}k\varphi)$ in the coordinate representation ($k = 0, \pm 1, \pm 2, \ldots$) and $|JK\rangle$ is a symmetric-top eigenfunction ($J = 0, 1, 2, \ldots, K = -J, \ldots, J$, and the M quantum number is omitted). The energy levels of free internal rotation of a symmetric top can be expressed as

$$E_{kJK}^{V=0} = ak^2 + BJ(J+1) + (A-B)K^2 + \alpha kK \tag{A3}$$

In the limiting case of a low barrier (small but nonzero $\hat{V}$), it is customary to use the eigenfunctions defined in Equation (A2) to represent $\hat{H}$ and its eigenfunctions, requiring the evaluation of the

$$\left\langle k'J'K'|\hat{H}|kJK\right\rangle = \left(E_{kJK}^{V=0}\delta_{k'k} + \left\langle k'|\hat{V}|k\right\rangle\right)\delta_{J'J}\delta_{K'K} \tag{A4}$$

matrix elements.

In the high-barrier limit, it is assumed that tunneling between the potential wells can be neglected; thus, it is sufficient to take into account one of the potential wells. Furthermore, the rovibrational energy-level formula corresponding to the high-barrier limit is derived within the framework of the HO approximation. Given these assumptions, one can expect that the spacings between the vibrational levels exceed those between the rotational levels; therefore, the rovibrational coupling term

$$\hat{W} = \alpha\hat{p}\hat{J}_z \tag{A5}$$

can be treated by perturbation theory. This procedure requires the evaluation of the matrix elements of $\hat{p}$ in the HO eigenbasis $|v\rangle$ ($v = 0, 1, 2, \ldots$). The nonzero HO matrix elements of $\hat{p}$ are

$$\langle v|\hat{p}|v+1\rangle = -\mathrm{i}\sqrt{\frac{m\omega}{2}}\sqrt{v+1} \tag{A6}$$

and

$$\langle v|\hat{p}|v-1\rangle = \mathrm{i}\sqrt{\frac{m\omega}{2}}\sqrt{v} \tag{A7}$$

where the vibrational mass is $m = \frac{1}{2a}$ and ω is the harmonic frequency.

The zeroth-order energy levels are

$$E_{vJK}^{(0)} = \omega\left(v+\frac{1}{2}\right) + BJ(J+1) + (A-B)K^2 \tag{A8}$$

and the zeroth-order eigenfunctions are defined as $|vJK\rangle$. The first-order energy correction is

$$E_{vJK}^{(1)} = \left\langle vJK|\hat{W}|vJK\right\rangle = \alpha K\langle v|\hat{p}|v\rangle = 0 \tag{A9}$$

as $\langle v|\hat{p}|v\rangle = 0$. The second-order energy correction can be expressed as

$$E_{vJK}^{(2)} = \sum_{v'\neq v}\frac{\left|\left\langle vJK|\hat{W}|v'JK\right\rangle\right|^2}{E_{vJK}^{(0)} - E_{v'JK}^{(0)}} = \frac{\alpha^2K^2}{\omega}\sum_{v'\neq v}\frac{|\langle v|\hat{p}|v'\rangle|^2}{v-v'} \tag{A10}$$

where it is sufficient to sum over v', as the matrix elements of $\hat{W}$ are diagonal in J and K. Considering the v=0 and $v \neq 0$ cases separately, we obtain

$$E_{0JK}^{(2)} = -\frac{\alpha^2K^2}{\omega}|\langle 0|\hat{p}|1\rangle|^2 = -\frac{m\alpha^2}{2}K^2 = -\frac{\alpha^2}{4a}K^2 \tag{A11}$$

and

$$E_{v\neq 0,JK}^{(2)} = \frac{\alpha^2K^2}{\omega}\left(|\langle v|\hat{p}|v-1\rangle|^2 - |\langle v|\hat{p}|v+1\rangle|^2\right) = -\frac{m\alpha^2}{2}K^2 = -\frac{\alpha^2}{4a}K^2 \tag{A12}$$

for the second-order energy-level correction. Note that $E_{vJK}^{(2)} = -\frac{\alpha^2}{4a}K^2$ for both cases.

APPENDIX B. The case of H_5^+ and D_5^+

In what follows, we apply the general results presented in Appendix A to characterize the torsion–rotation energy-level patterns of H_5^+ and D_5^+. Following Reference 51, the rotational constants are

$$A = \frac{1}{m_X r^2} \tag{B1}$$

and

$$B = \frac{1}{m_X\left(2R^2 + r^2\right)} \tag{B2}$$

using the parameters m_X (mass of H or D, X = H or X = D), r (distance between the two X atoms in the X_2 diatom), and R (distance of the two X_2 diatoms). The parameters a and α of Appendix A can be expressed in terms of A as $a = 2A$ and $\alpha = -2A$. We note that A, in contrast to B, is twice as large as its traditional rigid-rotor counterpart evaluated at the equilibrium structure.[51]

The zeroth-order torsion–rotation energy levels ($V = 0$ limit) are

$$E_{kJK}^{V=0} = 2Ak^2 + BJ(J+1) + (A-B)K^2 - 2AkK \tag{B3}$$

The energy-level formula of Equation (B3) gives rise to the degeneracy rules

$$E_{-k,J,-K}^{V=0} = E_{kJK}^{V=0} \tag{B4}$$

and

$$E_{K-k,J,K}^{V=0} = 2A(K-k)^2 + BJ(J+1) + (A-B)K^2 - 2A(K-k)K = E_{kJK}^{V=0} \tag{B5}$$

The torsional potential for H_5^+ (and D_5^+) can be represented accurately by the function

$$V(\varphi) = \frac{V_0}{2}(\cos(2\varphi) + 1) = \frac{V_0}{4}(\exp(\mathrm{i}2\varphi) + \exp(-\mathrm{i}2\varphi)) + \frac{V_0}{2} \tag{B6}$$

with $V_0 = 80.08\ \mathrm{cm}^{-1}$.[52] As the zeroth-order torsion–rotation energy-level pattern exhibits degeneracies and the torsional barrier is low, the effect of $V(\varphi)$ can be taken into account according to first-order degenerate perturbation theory, requiring the evaluation of the matrix elements

$$\langle k'J'K'|\hat{V}|kJK\rangle = \left(\frac{V_0}{2}\delta_{k'k} + \frac{V_0}{4}\left(\delta_{k',k+2} + \delta_{k',k-2}\right)\right)\delta_{J'J}\delta_{K'K} \tag{B7}$$

Based on Equation (B7), it is straightforward to see that only the zeroth-order eigenstates $|kJK\rangle$ and $|k'JK\rangle$ with $|k-k'| = 2$ give rise to nonzero interaction matrix elements.

Table B1 lists torsional energy levels for H_5^+ and D_5^+ with zero overall angular momentum ($J = 0$), and the numerically exact torsional energy levels $E^{V\neq 0}$ (employing nonzero torsional potential and coordinate-dependent torsional mass, see Reference 51 for computational details) are compared to their counterparts $E^{V=0}$ computed with the formula of Equation (B3) (zero torsional potential) and using the parameter values of $A = 53.34\ \mathrm{cm}^{-1}$, $B = 3.33\ \mathrm{cm}^{-1}$ for H_5^+ and $A = 26.69\ \mathrm{cm}^{-1}$, $B = 1.67\ \mathrm{cm}^{-1}$ for D_5^+, while J and K are set to zero. The degenerate $E^{V=0}$ pairs (with $k \neq 0$) are split if the torsional potential is taken into account. The $|k| = 1$ torsional energy-level pair exhibits by far the largest energy-level splitting, of $\Delta E^{V\neq 0} \approx 40\ \mathrm{cm}^{-1}$. This effect can be qualitatively understood by using first-order perturbation theory and the model potential of Equation (B6), implying that the degenerate zeroth-order levels with $|k| = 1$ are split by $V_0/2 = 40.04\ \mathrm{cm}^{-1}$ (the indeed much smaller splittings for $|k| > 1$ happen to be zero when this simple first-order perturbational model is used).

H_5^+				D_5^+			
$E^{V\neq 0}$	$\Delta E^{V\neq 0}$	$E^{V=0}$	k	$E^{V\neq 0}$	$\Delta E^{V\neq 0}$	$E^{V=0}$	k
0.00		0.00	0	0.00		0.00	0
87.93		106.67	−1	36.06		53.38	−1
128.26	40.33	106.67	1	76.29	40.23	53.38	1
429.10		426.70	−2	217.45		213.51	−2
429.35	0.25	426.70	2	219.55	2.10	213.51	2
962.17		960.06	−3	484.58		480.40	−3
962.23	0.06	960.06	3	484.65	0.07	480.40	3

TABLE B1 Torsional energy levels ($J = 0$) for H_5^+ and D_5^+. Energy levels are referenced to the ground-state torsional energy level (39.82 and 36.91 cm^{-1} for H_5^+ and D_5^+, respectively) and are given in units of cm^{-1}. The torsional quantum number k is used to label the zeroth-order energy levels $E^{V=0}$ (based on Equation (B3), with zero torsional potential energy). The energy levels $E^{V\neq 0}$ were computed by solving the torsional Schrödinger equation with nonzero torsional potential and coordinate-dependent torsional mass.[51] $\Delta E^{V\neq 0}$ specifies splittings between energy levels $E^{V\neq 0}$ corresponding to degenerate $E^{V=0}$ values

TABLE B2 Torsion-rotation energy levels ($J > 0$) for H_5^+. Energy levels are referenced to the ground-state torsional energy level and are given in units of cm^{-1}. The zeroth-order energy levels $E^{V=0}$ are labeled with the torsional quantum number k and projection quantum number K. The energy levels $E^{V\neq 0}$ were computed by solving the torsion-rotation Schrödinger equation with nonzero torsional potential and coordinate-dependent torsional mass[51]

$J = 1$				$J = 2$				$J = 3$				$J = 4$			
$E^{V\neq 0}$	$E^{V=0}$	k	K	$E^{V\neq 0}$	$E^{V=0}$	k	K	$E^{V\neq 0}$	$E^{V=0}$	k	K	$E^{V\neq 0}$	$E^{V=0}$	k	K
6.68	6.67	0	0	20.04	20.01	0	0	40.09	40.02	0	0	66.80	66.70	0	0
55.97	56.67	−1	−1	69.16	70.01	−1	−1	88.95	90.02	−1	−1	115.33	116.70	−1	−1
55.97	56.67	0	−1	69.16	70.01	0	−1	88.95	90.02	0	−1	115.33	116.70	0	−1
56.14	56.67	0	1	69.67	70.01	0	1	89.97	90.02	0	1	117.02	116.70	0	1
56.14	56.67	1	1	69.67	70.01	1	1	89.97	90.02	1	1	117.03	116.70	1	1
94.61	113.34	−1	0	107.96	113.34	−1	−2	127.99	133.35	−1	−2	154.69	160.03	−1	−2
134.95	113.34	1	0	113.35	113.34	1	2	133.37	133.35	1	2	160.02	160.03	1	2
273.41	270.02	−2	−1	113.36	126.68	−1	0	133.40	146.69	−1	0	160.13	173.37	−1	0
273.41	270.02	1	−1	148.33	126.68	1	0	168.43	146.69	1	0	195.25	173.37	1	0
273.45	270.02	−1	1	201.28	220.02	−2	−2	221.31	240.03	−2	−2	248.01	266.71	−2	−2
273.45	270.02	2	1	201.28	220.02	0	−2	221.31	240.03	0	−2	248.02	266.71	0	−2
435.78	433.37	−2	0	241.62	220.02	0	2	261.69	240.03	0	2	288.44	266.71	0	2
436.04	433.37	2	0	241.62	220.02	2	2	261.69	240.03	2	2	288.45	266.71	2	2
698.98	696.72	−3	−1	286.74	283.36	−2	−1	276.08	276.69	−2	−3	302.79	303.37	−2	−3
698.98	696.72	2	−1	286.74	283.36	1	−1	276.08	276.69	−1	−3	302.79	303.37	−1	−3
698.98	696.72	−2	1	286.86	283.36	−1	1	276.08	276.69	1	3	302.79	303.37	1	3
698.98	696.72	3	1	286.86	283.36	2	1	276.08	276.69	2	3	302.79	303.37	2	3
968.85	966.73	−3	0	449.15	446.71	−2	0	306.74	303.37	−2	−1	333.41	330.05	−2	−1
968.91	966.73	3	0	449.40	446.71	2	0	306.74	303.37	1	−1	333.42	330.05	1	−1
				542.46	540.04	−3	−2	306.98	303.37	−1	1	333.81	330.05	−1	1
				542.46	540.04	1	−2	306.98	303.37	2	1	333.81	330.05	2	1
				542.71	540.04	−1	2	469.20	466.71	−2	0	440.06	440.04	−2	−4
				542.71	540.04	3	2	469.46	466.71	2	0	440.06	440.04	2	4
				712.35	710.05	−3	−1	493.46	490.04	−3	−3	495.93	493.39	−2	0

(Continues)

TABLE B2 (Continued)

$J = 1$				$J = 2$				$J = 3$				$J = 4$			
$E^{V\neq 0}$	$E^{V=0}$	k	K	$E^{V\neq 0}$	$E^{V=0}$	k	K	$E^{V\neq 0}$	$E^{V=0}$	k	K	$E^{V\neq 0}$	$E^{V=0}$	k	K
				712.35	710.05	2	−1	493.46	490.04	0	−3	496.20	493.39	2	0
				712.35	710.05	−2	1	493.47	490.04	0	3	520.20	516.72	−3	−3
				712.35	710.05	3	1	493.47	490.04	3	3	520.20	516.72	0	−3
				982.22	980.07	−3	0	562.51	560.05	−3	−2	520.20	516.72	0	3
				982.28	980.07	3	0	562.51	560.05	1	−2	520.20	516.72	3	3
								562.76	560.05	−1	2	527.98	546.71	−3	−4
								562.76	560.05	3	2	527.98	546.71	−1	−4
								732.40	730.06	−3	−1	568.32	546.71	1	4
								732.40	730.06	2	−1	568.32	546.71	3	4
								732.40	730.06	− 2	1	589.24	586.73	−3	−2
								732.40	730.06	3	1	589.24	586.73	1	−2
								919.01	916.73	−4	−3	589.51	586.73	−1	2
								919.01	916.73	1	−3	589.52	586.73	3	2
								919.01	916.73	−1	3	759.13	756.74	−3	−1
								919.01	916.73	4	3	759.13	756.74	2	−1
												759.13	756.74	−2	1
												759.14	756.74	3	1
												869.16	866.73	−4	−4
												869.16	866.73	0	−4
												869.41	866.73	0	4
												869.41	866.73	4	4
												945.74	943.41	−4	−3
												945.74	943.41	1	−3
												945.75	943.41	−1	3
												945.75	943.41	4	3

When comparing the $\Delta E^{V\neq 0}$ values of H_5^+ and D_5^+, one can observe that the splittings are basically mass independent. This mass independence is in stark contrast to what one would expect if the torsion–rotation quantum dynamics of H_5^+ could be explained by tunneling between the two equivalent torsional potential wells. This observation, together with the extremely low torsional barrier, leads to the conclusion that the energy-level splittings can be attributed to the perturbation of a free internal rotor by a weak torsional potential; in other words, tunneling is not responsible for the torsional energy-level pattern of H_5^+.

Table B2 lists torsion–rotation energy levels for H_5^+ with $J > 0$. The clustering of the energy levels in Table B2 can be explained by the degeneracy rules derived for the zeroth-order energy-level pattern. Although most $E^{V\neq 0}$ values are in good agreement with their $E^{V=0}$ counterparts, there are some cases where the $E^{V\neq 0}$ values substantially deviate from the corresponding $E^{V=0}$ values and energy-level splittings of about $40\,\mathrm{cm}^{-1}$ occur. By inspecting the quantum numbers k and K in Table B2, one can notice that the $\Delta E^{V\neq 0} \approx 40\,\mathrm{cm}^{-1}$ splittings are always observed for zeroth-order eigenstates $|kJK\rangle$ and $|k'JK\rangle$ with $|k - k'| = 2$. Therefore, this effect can also be interpreted with the first-order perturbational treatment used to qualitatively explain the $J = 0$ torsional energy-level pattern.

Finally, we note that if the torsion–rotation energy-level patterns of H_5^+ were described with the high-barrier formalism, one would get the second-order energy-level correction

$$E_{vJK}^{(2)} = -\frac{\alpha^2}{4a}K^2 = -\frac{A}{2}K^2 \tag{B8}$$

therefore, the torsion–rotation energy levels up to second order would read as

$$E_{vJK}^{[2]} = E_{vJK}^{(0)} + E_{vJK}^{(2)} = \omega\left(v+\frac{1}{2}\right) + BJ(J+1) + \left(\frac{A}{2}-B\right)K^2 \tag{B9}$$

One can observe immediately that the last term of Equation (B3), linear in K, is eliminated and, instead of A, $A/2$ appears in Equation (B9). As a result, the usual RRHO energy-level formula is recovered using the high-barrier formalism.